

## Reservoir Characterization and Estimation of Hydrocarbon Reserves of OJ-Field, Onshore Niger Delta, Nigeria

†Boboye, O.A. and Otelaja, O.J.

### Abstract

The reservoir characterization of OJ-Field in the eastern onshore of Niger Delta was determined using 3-D seismic and well logs data. The main objectives are to access the potential reservoir sands with parameters that control its hydrocarbon distribution, fluid type, identify structures necessary for hydrocarbon accumulation and estimation of hydrocarbon reserves. Structural maps of horizons in four wells containing hydrocarbon bearing zones with tops and bases at subsea depth range of -6723.93 to -9678.46ft were produced, showing the trapping mechanism to be mainly fault-assisted roll-over structures. From the four reservoir sands delineated, Sand A (-6723.93 to -7143.18ft) is the most prolific hydrocarbon bearing with 56.07MMbbl of oil and recoverable reserve of 6.46MMbbl while Sand C (-8343.37 to -9203.15ft) is the second most prolific reservoir sand with 49.68MMbbl of oil and recoverable reserve of 11.92MMbbl. Sand\_D (-8471.83 to -9678.46ft), which is the second least prolific, has 31.17MMbbl of oil, 112.74MMcf of gas and 0.94MMbbl recoverable reserve while the least prolific, Sand\_B (-7181.12 to -7877.56ft), contain 26.05MMbbl of oil with recoverable reserve of 5.25MMbbl. Also, OJ-01 well was the most promising of all the wells considered with 65.96MMbbl of oil and recoverable reserve of 5.21MMbbl compared with OJ-02 having 42.91MMbbl of oil and recoverable reserve of 13.63MMbbl. OJ-04 is equally productive with 40.58MMbbl and 112.74MMcf of oil and gas respectively with recoverable reserve of 3.77MMbbl while OJ-03 is the least promising well with 13.52MMbbl of oil that yielded recoverable reserve of 1.96MMbbl. The total net volume of the reservoirs yielded stock tank oil in place of 162.98MMbbl and gas in place of 112.74MMcf. Only, 24.58MMbbl can be recovered from the stock tank oil in place estimated and this is attributed to insufficient drive mechanism and high viscosity.

**Key words:** Fault, Hydrocarbon, Net volume, Reservoir, Stock Tank Oil in Place, Viscosity.

### Introduction

The prolific demand for hydrocarbon products since the 20<sup>th</sup> century prompted and intensified exploration for oil and gas accumulation in reservoir rocks. This led to an extensive study of the Niger Delta depocenters after a long while of non-productive search in the Cretaceous sediments of the Benue Trough [1].

Petroleum in the Niger Delta is produced from sandstones and unconsolidated sands predominantly in the Agbada Formation which is the major oil-producing in the Niger Delta Complex Basin [1]. Recognized known reservoir rocks are of Eocene to Pliocene in age and are often stacked, ranging in thickness from less than 15m to 10% having greater than 45m thickness [2]. Based

on reservoir geometry and quality, the lateral variation in reservoirs thickness is strongly controlled by growth faults; with the reservoirs thickening towards the fault within the down-thrown block [3]. This study is aimed at using available geophysical data to determine the volume capacity of each of the promising reservoir sands within 'OJ-Field', located on east onshore of Niger Delta. The geometry of the reservoir which includes the area extent, structure and thickness will be determined by seismic data and well calibration while the lithologies present will be identified and correlated in the well section. Also, the fluid in the reservoir will be defined by bulk rock volume combined with porosity distribution. The fluid types depend to a large extent on the fluid contacts and to a less extent on petrophysical properties. Petrophysical properties such as porosity, permeability, water saturation and net to gross, will be determined from the well logs.

---

†Boboye, O.A. and Otelaja, O.J.

†Department of Geology, University of Ibadan, Ibadan, Nigeria.

E-mail: oa.boboye@mail.ui.edu.ng,  
fmotelaja@yahoo.com

Structural map will be generated via faults and horizons mapped in order to calculate the petrophysical and volumetric properties of the delineated reservoirs.

**Location of Study Area**

‘OJ-Field’ is located within the OML 17, east onshore of Niger Delta between latitude 5°00N – 5°30N and longitude 6°30E –

7°00E with a rectangular area of 46.08sq.km. The co-ordinates were generated from the Niger Delta concession map while the area was calculated using Petrel 2009.1 software (Figs. 1 and 2). The field is characterized by faults that bordered it and from the fault analysis, they are found to be sealing; hence, they are called ‘boundary faults’.

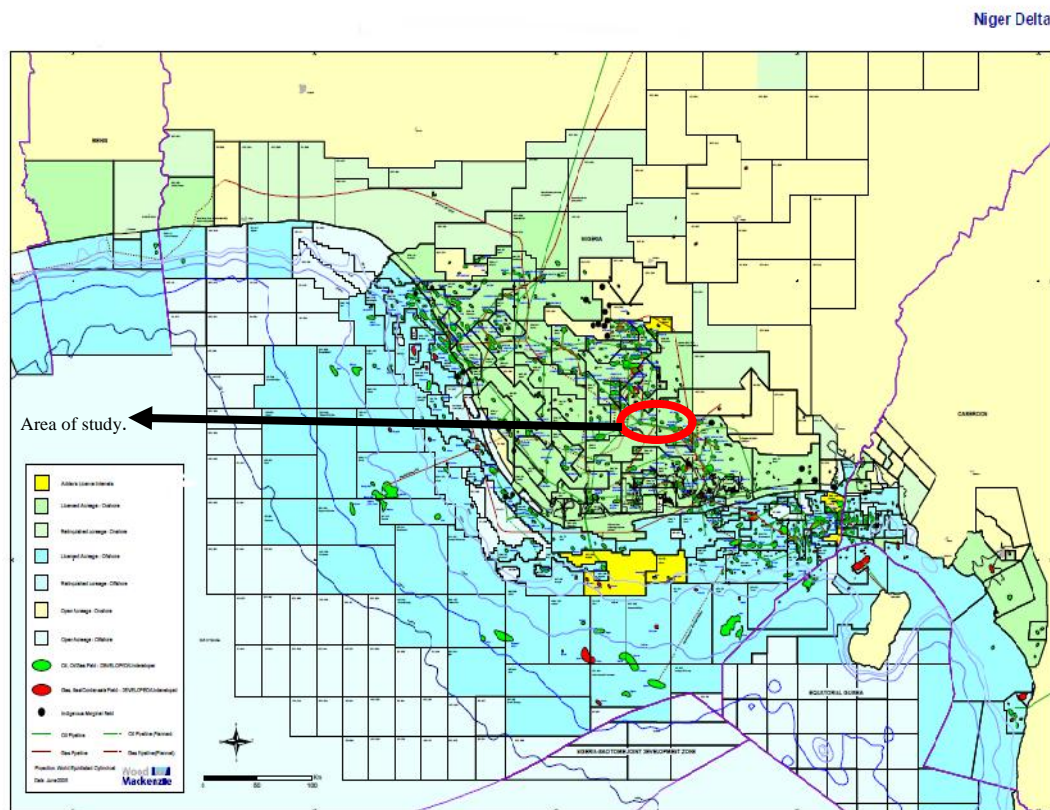


**Fig. 1:** Concession map of Niger Delta showing the area of study.

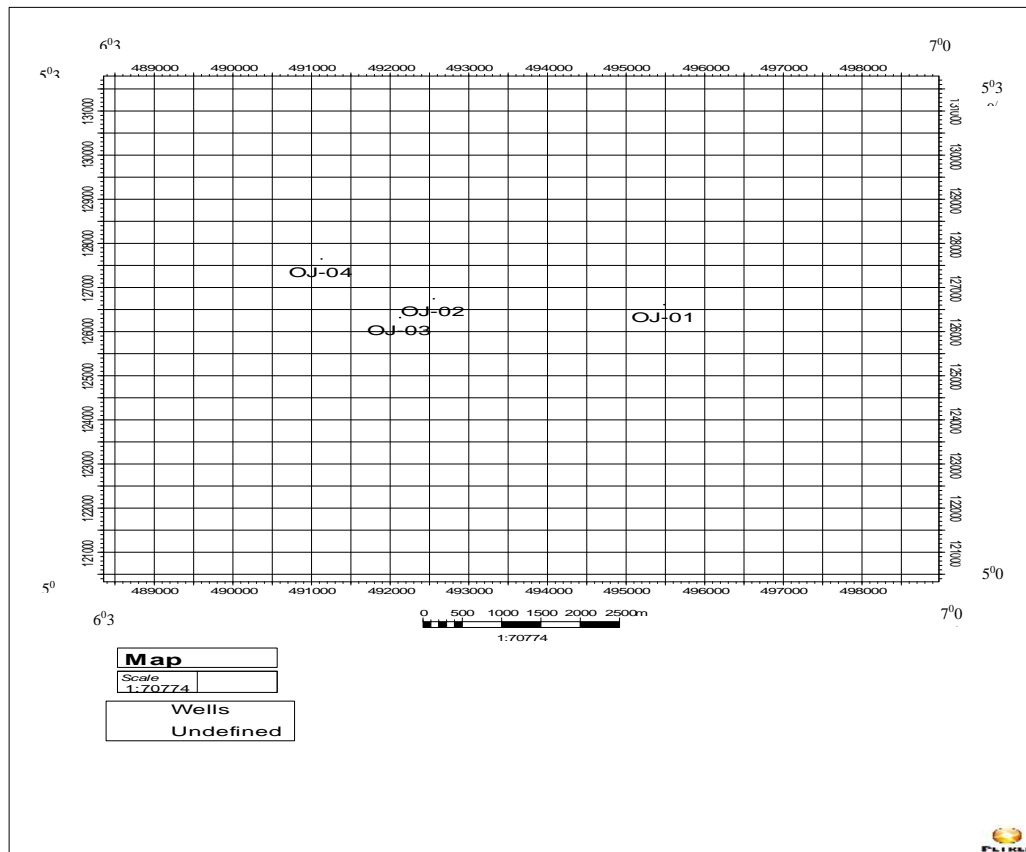


Fig. 2: The base map of ‘OJ-Field’ showing the wells’ locations.

**Previous Work**

The Niger Delta Basin is situated on the continental margin of the Gulf of Guinea in equatorial West Africa of latitude 3<sup>0</sup> and 6<sup>0</sup> N and longitude 5<sup>0</sup> and 8<sup>0</sup> E. It is one of the largest regressive deltas in the world [1] and is considered a classical shale tectonic province [4]. The onshore portion of the Niger Delta Province is delineated by the geology of southern Nigeria and southwestern Cameroon. The northern boundary is the Benin flank—an east-northeast trending hinge line south of the West Africa basement massif. The northeastern boundary is defined by outcrops of the Cretaceous on the Abakaliki High and further east-south-east by the Calabar flank—a hinge line bordering the adjacent Precambrian. The offshore boundary of the province is defined by the Cameroon volcanic line to the east, the eastern boundary of the Dahomey Basin to the west, and the

two kilometer sediment thickness contour or the 4000m bathymetric contour in areas where sediment thickness is greater than two kilometers to the south and southwest. The shape and internal structure of the Niger Delta are also controlled by fracture zones along the oceanic crust, such as the Charcot fracture zone, expressed as trenches and ridges that were formed during the opening of the South Atlantic in the Early Jurassic–Cretaceous. The province covers 300,000 km<sup>2</sup> and includes the geologic extent of the Tertiary Niger Delta (Akata-Agbada) Petroleum System.

Several workers have carried out research on Niger Delta basin reservoir with special emphasis on geometry, hydrocarbon distribution and quantification. Weber and Daukoru [3] described the lateral variation in the thickness of the reservoir to be strongly controlled by growth faults and the reservoir

grows thicker towards the faults within the down-thrown block. Avbovbo [5] believed that Agbada Formation which is the reservoir rock in Niger delta consists of paralic sequence of sandstone and shale intercalations. Ejedawe [6] related the position of the oil-rich areas within the belt to five delta lobes fed by four different rivers. He also stated that the two controlling factors are an increase in geothermal gradient, relative to the minimum gradient in the delta center and the generally greater age of sediments within the belt relative to those further seaward. Weber indicated that the oil-rich belt (“golden lane”) coincides with a concentration of rollover structures across depobelts having short southern flanks and little paralic sequence to the south [7].

Doust and Omatsola [1] also reported that Agbada Formation forms the hydrocarbon prospective zone of the Niger delta that is the thicker reservoirs likely represent composite bodies of stacked channels. Edwards and Santogrossi [8] described the primary Niger Delta reservoirs as Miocene paralic sandstones with 40% porosity, 2000 millidarcys permeability, and thickness of 100m. Ekweozor and Daukoru, [9] noted that sandstone reservoirs contained within the Agbada Formation are a mixture of barrier bars and channel sands with occasional deep water turbidites in the transitional sequence into the Akata Formation. Beka and Oti, [10] reported that in the outer portion of the delta complex, deep sea channel sands, lowstand sand bodies, and proximal turbidites create potential reservoirs.

Kulke described the most important reservoir type in the Niger delta as point bars distributory channels and coastal bars intermittently cut by sand-filled channels, based on the reservoir geometry and quality, and that many reservoirs are overpressured and primary production is mainly from gas expansion [11]. Stacher stated that faulting in the Agbada Formation provided pathways for petroleum migration and formed structural traps that, together with stratigraphic traps,

accumulated petroleum [12]. Smith-Rouch and other workers showed that local fault movement along slope edge controls thickness and lithofacies of potential reservoir sands downdip [13].

### **Stratigraphy**

The Niger Delta Basin consists of Cretaceous to Holocene marine clastic strata that overlie oceanic and fragments of continental crust [14]. The Cretaceous section has not been penetrated beneath the Niger Delta Basin, and thus, Cretaceous lithologies can only be extrapolated from the exposed sections in the next basin to the northeast, the Anambra Basin. In this basin, Cretaceous marine clastics consist mainly of Albian–Maastrichtian shallow-marine clastic deposits [15, 16]. The precise distribution and nature of correlative Cretaceous deposits beneath the offshore Niger Delta is unknown. From the Campanian to the Paleocene, both tide dominated, and river-dominated deltaic sediments were deposited during transgressive and regressive cycles, respectively [16]. In the Paleocene, a major transgression initiated deposition of the Imo shale in the Anambra Basin and the Akata shale in the Niger Delta Basin and during the Eocene, the sedimentation changed to being wave dominated [16]. At this time, deposition of paralic sediments began in the Niger Delta Basin, and as the sediments prograded south, the coastline became progressively more convex seaward. Today, delta sedimentation remains wave dominated [1].

The Tertiary section of the Niger Delta is divided into three formations, representing prograding depositional environments. The type sections of these formations have been described [1, 2, 5, 11, and 17]. The Akata Formation at the base of the delta is of marine origin, and its thickness ranges from 2000 m (6600 ft) at the most distal part of the delta to 7000m (23,000 ft) thick beneath the continental shelf [1]. In the deep-water fold and thrust belts, the Akata Formation is up to 5000 m (16,400 ft) thick because of structural

repetitions by thrust ramps and in the core of large detachment anticlines [18]. The Akata Formation is composed of thick shale sequences that are believed to contain source rocks and may contain some turbidite sands (potential reservoirs in deep-water environments). On seismic sections, the Akata Formation is generally devoid of internal reflections [19], with the exception of a strong, high-amplitude reflection that is locally present in the middle of the formation. This mid-Akata reflection serves as an important structural marker for defining detachment levels. The Akata exhibits low P-wave seismic velocities ( 2000 m/s; 6600 ft/s) that may reflect regional fluid overpressures [20].

Deposition of the overlying Agbada Formation, the major petroleum-bearing unit in the Niger Delta, began in the Eocene and continues into the present. The Agbada Formation consists of paralic siliciclastics more than 3500 m (11,500 ft) thick and represents the actual deltaic portion of the sequence. This clastic sequence was accumulated in delta-front, delta-topset, and fluviodeltaic environments. Channel and basin floor fan deposits in the Agbada Formation form the primary reservoirs in the Niger Delta. Onshore and in some coastal regions, the Agbada Formation is overlain by the Benin Formation, which is composed of Oligocene to Recent continental deposits, including alluvial and upper coastal-plain deposits that are up to 2000 m (6600 ft) thick [5].

### Local Geology of the Study Area

The classic Niger Delta sand-shale succession of the major lithostratigraphic units; Benin, Agbada and Akata are evident in the eastern flank of the delta. However, only the Benin Formation and transitional Agbada Formation were penetrated by wells in 'OJ-Field'. The Benin Formation in the main 'OJ-Field' area covers the interval from seabed to approximately -6500ft *tvds*. It is a massive fresh-water bearing sequence of upper delta plain sands and gravels interbedded with soft,

sticky grey clays and lignite. The finer-grained beds are not continuous but there appears to be a more extensive interval of interbedded shales and sands (Agbada Formation) at approximately -6700ft *tvds*. The Akata Formation consists of prodelta shales and it has not been penetrated in 'OJ-Field' but it is estimated to be at depth of approximately -12,000ft *tvds*, far below the deepest penetration point in the field (-9730ft *tvds* in OJ-02).

### Stratigraphic and Structural Framework

The three formations of the Niger Delta can be identified on the seismic sections of the 'OJ-Field' area. The region on the seismic section where faults can be observed i.e. the growth section from 1500-3000ms is identified as the Agbada Formation. The region beneath this growth section i.e. the pre-growth section is the Akata Formation. On the section, the reflections of this portion are not so clear and appear to be hummocky, which is probably due to the abundance of shales which cannot really be classified as independent parallel sequences as in the case of sands or intercalations of sands and shales. The abundance of marine shales in the pre-growth section lends credibility to this hypothesis. The uppermost portion of the section coincides with the Benin Formation, 0-1500ms and is characterized by clear, parallel, undeformed reflections. Channel-like features have been observed in the 'OJ-Field' area on all the crossline but on no inline section. This is because the crossline is along the cross section of the channel and the feature would have a rough V-shape for steeply gradient and U-shape for gentle slope on the section, while the inline section is perpendicular and only the channel path and its fill can be observed in this perspective and not the cross-sectional shape of the feature. A series of channels occur in the range of 2700-3300ms on all the crosslines. This indicates extensive activity of the fluvial system during this period.

The predominant faulting style in the 'OJ-Field' area is the listric style of deformation.

The major faults in the area are listric shaped growth faults, the largest of which extends from 1500 – 3000ms on the seismic section. This range coincides with the growth section in the area and all faults observed fall within this two-way time range. The listric faulting style indicates that the ‘OJ-Field’ area is probably in the onshore area of the Niger Delta, moreover the relatively simple faulting pattern as opposed to collapsed crests, shale diapirism and back-to-back faulting indicates that the area is not in the offshore areas. The area is characterized by simple listric shaped growth faults of which there are 2 major ones, 2 minor non-growth faults and 2 antithetic faults. The structure of the area dips towards the south with an increase in depth across two major downthrown blocks bounded by 2 major growth faults – F<sub>1</sub> and F<sub>2</sub> faults that define the southern limits of the area. There is no available data beyond the southern part of the faults. There is a third downthrown block at the extreme southwest to the antithetic F<sub>3</sub> fault, which extends beyond the southern fringes of the ‘OJ-Field’ area. There is structural high in each of the major downthrown blocks—one three-way closure to the eastern part of the downthrown block closing in on the thinner portion of the major black fault. Due to the smaller growth and heave values of the F<sub>1</sub> fault at the eastern portion where it starts to grow compared to the northern portion where it has achieved maximum growth, there is risk that any hydrocarbon trapped in the closure of the high at the west of the fault may leak through the smaller and less secure fault trap. The second high is a three-way closure in the block upthrown to the black fault but downthrown to the major northern pink fault.

### **Materials and Methods**

The data for this study was provided by Shell Petroleum and Development Company

Limited. The data set includes well logs, 3D survey data and check shot data of four different widely spaced vertical wells from ‘OJ-Field’, onshore Niger Delta. These data were combined and analyzed using Schlumberger’s Petrel 2009.1 version software. Also, the data were validated, imported and edited to reduce error. Interpretation started with well log data by choosing hydrocarbon bearing sands using gamma ray and resistivity log and their east-west correlation in the wells in the cross section [21, 22]. The wells’ positions relative to one another are: OJ-01, OJ-02, OJ-03 and OJ-04. The main physical parameters necessary for reservoir evaluation were inferred from log signatures. Consequently, the well logs were interpreted to determine the various lithologies, formation thickness while petrophysical parameters such as porosity, permeability, water saturation, hydrocarbon saturation and volume of shale were calculated using appropriate formula.

### ***Interpretation Techniques***

Both qualitative and quantitative techniques were integrated in this study. Qualitative interpretation includes the lithologic identification, stratigraphic relationship and formation thickness. The quantitative interpretation includes the calculation of porosity ( ), hydrocarbon saturation (Sh), formation water resistivity (Rw), permeability (k), water saturation (Sw), shale volume (Vsh), bulk volume water (BVW) and reserve estimation. The amount of hydrocarbon contained in a unit volume of the reservoir is a product of its porosity and hydrocarbon saturation. The quick look and conventional interpretation techniques were used, which make use of porosity, resistivity and lithology logs (Figs. 3, 4 and 5).

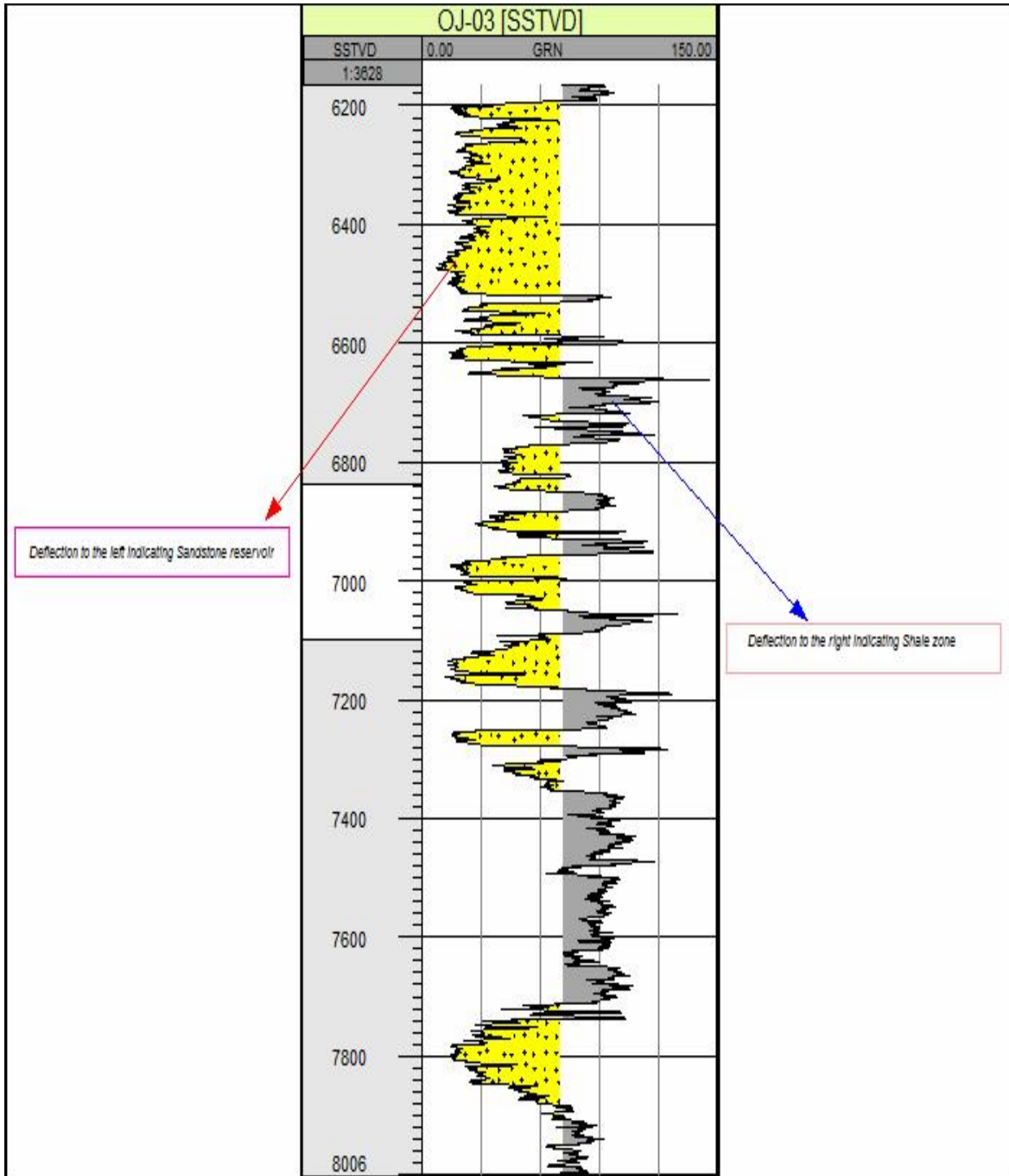


**Fig. 3:** Gamma ray log deflection analysis of well OJ-03 to indicate sandstone and shale lithologies.

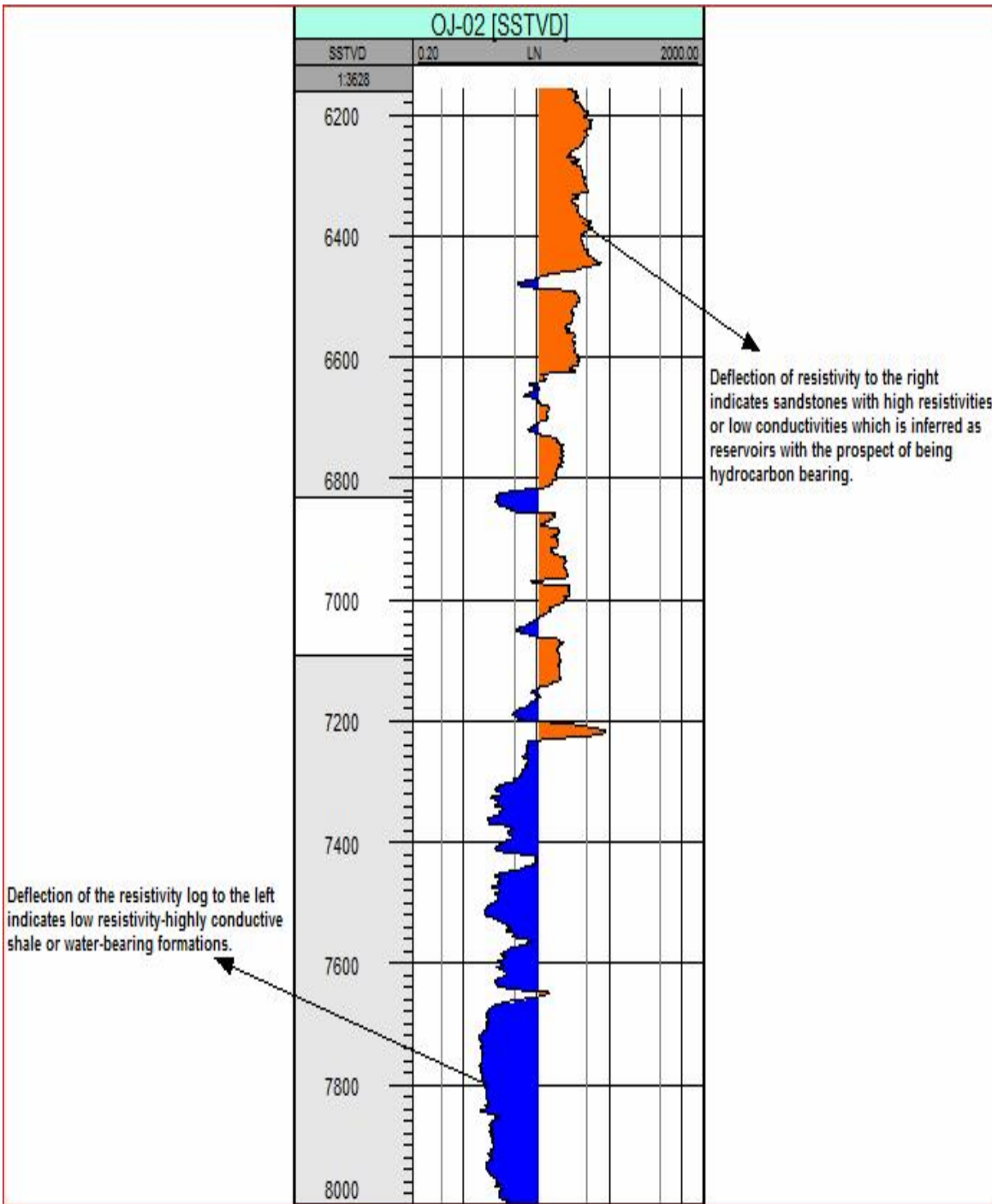


**Fig. 4:** Resistivity log deflection of well OJ-02 indicating water and hydrocarbon bearing zone.

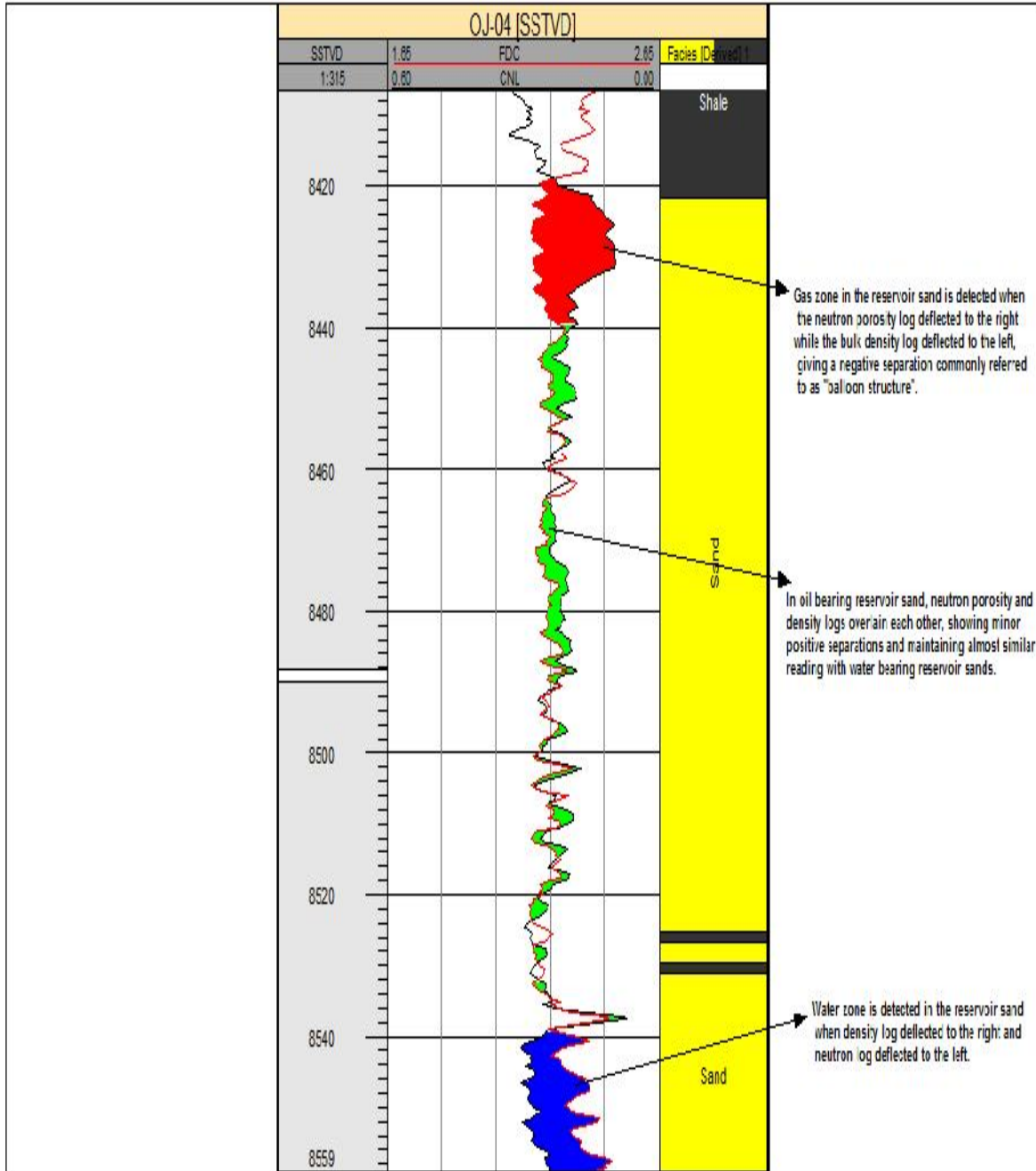


**Fig. 5:** Neutron-density porosity logs of well OJ-04 indicating the zones of gas, oil and water.

**Porosity Determination**

Porosity logs were used to calculate the formation total and effective porosities. It is the pore volume per unit volume of the formation and also, it is the fraction of the total volume of a sample that is occupied by

pores or voids. Porosity can be expressed in bulk density units (g/cm<sup>3</sup>) or percentage. The bulk density porosity is the overall gross or weight average density of a unit of the formation and it can be used as total porosity if it is only present. It is expressed by:

$$D = \frac{m_a - b}{m_a - f_l} \dots\dots\dots (1)$$

where,  $m_a$  = matrix density;  $b$  = bulk density read from the log;  
 $f_l$  = density of the fluid

• *From Neutron log*

This is read straight from the log and converted to percentage. The log is calibrated in linear function from 0.60 to 0.00 and since the log is recorded in apparent limestone, it

must be corrected for using appropriate chart, into sandstone. The combination of porosity derived from neutron and density logs give more accurate and effective porosity for calculation. The formula used is given as:

$$total = \frac{N + D}{2} \dots\dots\dots (2)$$

where,  $total$  = Porosity derived from the combination of neutron and density porosities  
 $N$  = Porosity derived from neutron log;  $D$  = Porosity derived from density log

• *From Sonic log*

Porosity can also be derived from sonic log through the use of time average relation

which is determined by applying the expression:

$$= \frac{t_{log} - t_{ma}}{t_f - t_{ma}} \dots\dots\dots (3)$$

where,  $t_{log}$  = transit time read from well log;  
 $t_{ma}$  = transit time of the matrix material,  
 $t_f$  = transit time of the saturating fluid

The value of  $t_f$  used for this study is 188.98µs/ft,  $t_{ma}$  for sandstone is 55.5µs/ft,  $t_{ma}$  for limestone is 47.6µs/ft, and  $t_{ma}$  for dolomite is 43.5µs/ft.

water. It is generally assumed, unless otherwise known that the pore volume not filled with water is filled with hydrocarbon. This could be determined mathematically or by using appropriate charts.

**Determination of water saturation (Sw), resistivity of the formation water (Rw) and hydrocarbon saturation (Sh)**

Water saturation (Sw) is the fraction of the pore volume of the reservoir that is filled with

The determination of water saturation is to compute the resistivity of the formation water (Rw) values which were determined from porosity-resistivity cross plot from 100% water saturation line. After which Rw value is substituted in the formula:

$$(S_w)^2 = \frac{a \cdot R_w}{R_t} \dots\dots\dots (4)$$

in hydrocarbon bearing zone.

where,  $S_w$  = Water saturation;  $R_w$  = Resistivity of the formation water;  
 $R_t$  = True resistivity measured from the deep resistivity log (un invaded zone);  
 = Porosity  
 $a$  = constant and is equal to 0.81

Also,  $\frac{a}{2}$  is referred to as Formation factor,  $F$ .

Moreover, hydrocarbon saturation ( $S_h$ ) can be derived from water saturation ( $S_w$ ) by using the formula:

$$S_h = 1 - S_w \dots\dots\dots (5)$$

**Determination of Irreducible Water Saturation, Permeability and Bulk Volume Water**

In a water wet formation, there is always a certain amount of water held in the pores by

capillary force. This water cannot be displaced by oil at pressures encountered in formations, so the water saturation never reaches zero. This Irreducible water saturation ( $S_{wirr}$ ) is given by:

$$(S_{wirr})^2 = \frac{F}{2000} \dots\dots\dots (6)$$

where,  $F$  = Formation factor

Several equations have been proposed in order to estimate permeability from measurements of porosity and irreducible water

saturation, but that proposed by Timur and documented by Dresser Atlas (1982) is found to be convenient:

$$K = \frac{0.136 * e^{4.4}}{S_{wirr}^2} \dots\dots\dots (7)$$

The bulk volume water (BVW) is determined from the product of water saturation and porosity.

$$BVW = e * S_w \dots\dots\dots (8)$$

$e$  = Effective porosity (i.e.  $e = e_{total} * (1 - V_{sh})$ )

If a formation of bulk volume water values are constant; or nearly constant then, it is at irreducible water saturation but if the values are widely varied, then it is not at irreducible water saturation. It is also important to know the effect of grain size on water saturation. If bulk volume of water is greater than or equal

to 0.09 ( 0.09), it is fine-grained sand, if it is greater than or equal to 0.06 ( 0.06), it is medium-grained sand while greater than or equal 0.04 ( 0.04), it is coarse-grained sand. From this bulk volume of water, the bulk volume of hydrocarbon (  $e * S_h$ ) was determined with equations 5 and 8 as well as

$$e * S_h = e * (1 - S_w) \dots\dots\dots (9)$$

$$BVH = e * S_h \dots\dots\dots (10)$$

where, BVH = Bulk Volume of hydrocarbon;  $e$  = Effective Porosity;  $S_h$  = Hydrocarbon Saturation.

**Determination of Volume of Shale (Vsh)**

Shale content, or volume of shale, is an important quantitative result of log analysis. It is needed for correcting porosity and is an indicator of reservoir quality. Lower shale content usually indicates a better reservoir

[23]. However, volume of shale was calculated through the gamma ray method as would be shown below. Shale volumes obtained for the reservoirs were used to correct porosity values [24].

$$I_{GR} = \frac{(GR_{log} - GR_{min})}{(GR_{max} - GR_{min})} \dots\dots\dots (11)$$

where,  $I_{GR}$  = Gamma ray index;  $GR_{log}$  = Gamma ray reading of the formation  
 $GR_{min}$  = Minimum Gamma ray (clean sand);  $GR_{max}$  = Maximum Gamma Ray (Shale)

The volume of shale is then calculated from the gamma ray index ( $I_{GR}$ ) by using the Dresser Atlas Formula:

$$V_{sh} = 0.083[2^{(3.7 \times I_{GR})} - 1.0] \dots\dots\dots (12)$$

For Tertiary unconsolidated rocks like those in Niger Delta. The Volume of Shale,  $V_{sh}$ , was then used to obtain the effective porosity ( $e$ ) in connection with total porosity ( $e_{total}$ ).

$$e = e_{total} * (1 - V_{sh}) \dots\dots\dots (13)$$

**Correlation of Reservoir Sands**

The sequential arrangement of the well logs was obtained from the base map of the area showing the positions of the wells (Fig. 2). The lithologic units were delineated in vertical succession by distinct surfaces which represent changes in lithologic character. The units were marked on the logs with the same identification mark and the process continued over the entire length of each log until all recognizable correlation units were identified.

Based on the two logs (gamma ray and resistivity) sand tops and the base of petrolific zones were picked and each of the formation tops and base were differentiated by assigning them name and color codes. This is to determine the lithologic successions, show regressive and/or transgressive sequences and the different sedimentary sand types deposited in the field or region (Fig. 6).

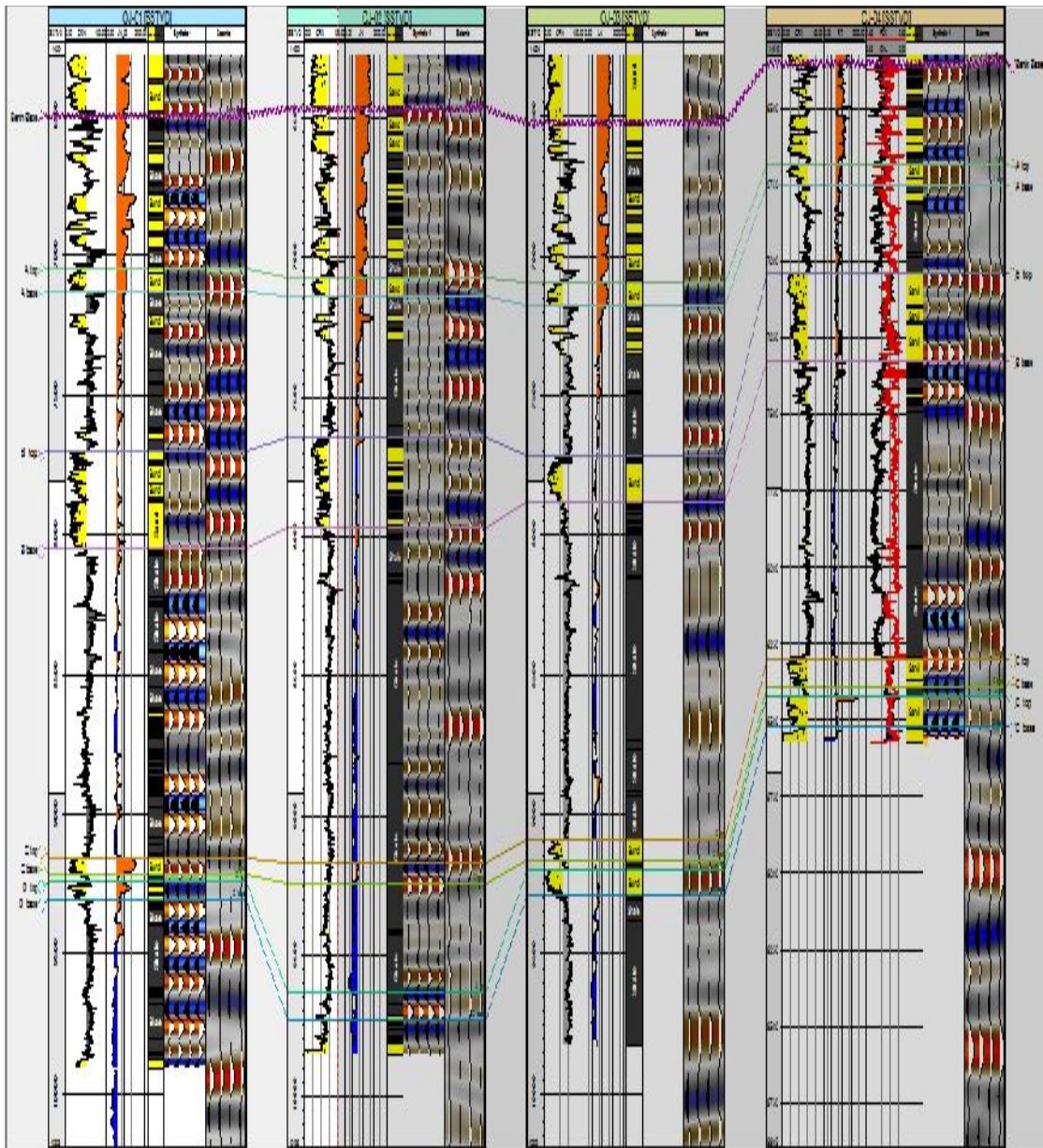


Fig. 6: Well logs correlation of the OJ-field, Onshore Niger Delta.

**Log depth measurements**

The measured depth (MD), true vertical depth (TVD), true vertical thickness (TVT) and subsea true vertical depth (SSTVD) of each lithofacies identified were calculated. For vertical holes, the MD and TVD are the same. In carrying out these measurements, the top and bottom depth values of the horizons were

read off directly from the well logs and this corresponds to the measured depth. To obtain SSTVD, the Kelly Bushy value was subtracted from the measured depth from the top to the bottom of each of the horizons. The difference between the top and bottom of SSTVD values obtained corresponds to the TVT (Fig. 7).

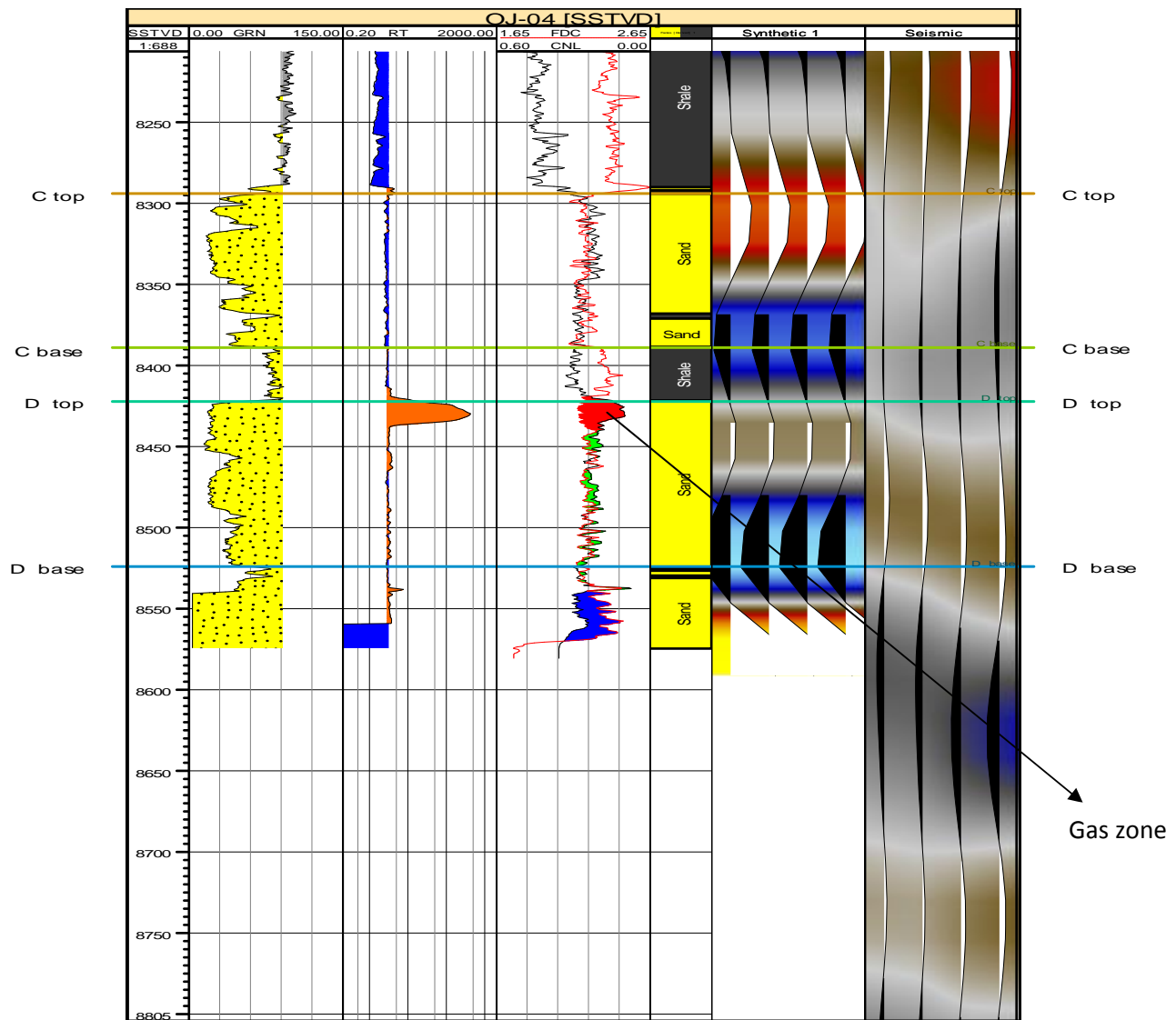


Fig. 7: OJ-04 well showing the gas zone at reservoir Sand\_D.

**Reserve Estimation**

The volume of hydrocarbon producible from a reservoir is a function of its thickness and area. Porosity and saturation (oil) is equally important since they vary both laterally and vertically. The reservoir thickness is the same as its height, *H*. The thickness was determined from the log, measured in feet and the area in acre was determined from the depth structural map using petrel algorithm. Therefore, deterministic estimation of the

volume of hydrocarbon in place involves the application of one or more simple equations that describes the volume of hydrocarbon filled pore space in the reservoir and the way that volume will change from the reservoir to the surface. We considered the weighted mean hydrocarbon saturation of the net pay section and estimated the hydrocarbon in place and this quantity is the Oil Initially In Place (OIIP).

$$OIIIP = GRV \times N/G \times (1 - Sw) \dots\dots\dots (14)$$

where, GRV is the Gross Rock Volume; N/G is the net to gross (interval ratio) is the porosity and Sw is the water saturation.

OIIP was converted into recoverable reserve in terms of Stock Tank Oil In Place (STOIP) by applying an additional factor.

$$STOIP = [7758 \times GRV \times N/G \times (1 - Sw)]/Boi \dots\dots\dots (15)$$

where, Boi is the oil formation volume factor and it is estimated from the production data.

This parameter is essential for converting oil volumes from reservoir to stock tank conditions. Boi is obtained from Pressure-Volume-Temperature (PVT) analysis in the laboratory and its most common range is 1.10 - 1.6 but 1.2 value was used for this study.

Recoverable reserve (N) is given as:

$$N = STOIP \times RF \dots\dots\dots (16)$$

where, RF is the Recovery factor and it depends on drive mechanism, permeability, reservoir depth and hydrocarbon viscosity.

Also, gas in place, GIP was also estimated by using this equation:

$$GIP = [43560 \times GRV \times N/G \times Sg] / Bg \dots\dots\dots (17)$$

where, Sg is the gas saturation; Bg is the gas formation volume factor

**Seismic Interpretation of Reflection Data**

Seismic data interpretation started with a general overview of the seismic sections to understand general subsurface geology related to the field’s evolution. The seismic data consist of a series of cross-lines and in-lines and to cover the study area, it was interpreted at a scroll of 10 lines on both cross-lines and in-lines. For valid interpretation, well log data were tied with seismic data using the check shot information. Horizons were also mapped and each mapping of the horizons ended in a loop, for ensuring correctness of interpretation and a 3D image of the reservoir. Fault mapping was carried out first to guarantee that horizons mapped reckon with general framework in the area.

**Fault Mapping**

Each of the observed faults on the in-line sections were marked with a colour line. They were recognized in portions where there is a change in the dip reflections, or a break of reflections in a downward direction. The points where the faults cross the cross-lines were posted onto the cross-lines to give the shape of the fault in the strike direction, (this procedure acted as a quality control of the faults marked on the In-lines), because a fault present on an In-line must also occur on the cross-lines without breaking through continuous reflections. Interestingly, the same fault has different shapes on In-line and cross-lines while observing the fault along the dip and strike orientations respectively. Also on the In-lines, it is observed that as a fault grows longer, the throw of the fault gets

larger—this is a characteristic of growth faults in the Niger Delta region.

The faults were posting on the cross-lines and a nomenclature was assigned to each fault based on colours. This act established the presence of the faults although minor editions had to be performed on the faults during the next quality control procedure – Horizon Mapping.

### ***Horizon Mapping***

Prolific reservoir sand horizons were detected by the use of logs and checkshot data from all the wells. Four horizons were delineated for mapping.

- Sand\_A at -6723.93ft (-2049.45m) to -7088.74ft (-2160.65m) TVDSS
- Sand\_B at -7181.12ft (-2188.81m) to -7877.56ft (-2401.08m) TVDSS
- Sand\_C at -8343.37ft (-2543.06m) to -9203.15ft (-2805.12m) TVDSS
- Sand\_D at -8471.83ft (-2582.21m) to -9678.46ft (-2950m) TVDSS

The reservoir sands were tied to the equivalent horizons visible as reflections on the seismic sections. The top of the sand horizons were mapped with coloured line and carried along all sections and across all faults. After the sand horizons had been mapped on all sections, both In-lines and Cross-lines, each In-line was crossed with its complimentary Cross-line at each point to make sure the mapped horizons were the same all through the sections (This acted as quality control).

Two-way travel time values were measured at each grid point from the 0 ms mark to the targeted horizon. The values were posted onto the grid map at the appropriate points. In addition, all points on all sections, where faults cut the targeted horizons were posted onto the map indicating the position of the faults and their direction of dip. After posting the two-way travel time values and fault positions onto the map, the two-way travel time was converted to depth and all

points of equal value were contoured to produce depth structure maps of the Sands\_A, B, C, and D horizons. These depth values were contoured between 50ft (15.2m) and 80ft (24.2m) interval to give a concise representation of the structures in depth and the area derived was used for volumetric calculations.

## **Results and Discussion**

### ***Petrophysical Evaluation***

The parameters of the potential reservoir sands within the four wells were calculated and the results signify that identified sands occurring at subsea depths of -6723.93ft (-2049.45m) to -9678.46ft (-2950m) have excellent petrophysical values with enormous reserves. All the reservoirs' gross interval ranges from 56.99ft (17.37m) to 336.73ft (102.64m), gross volume of 197255.92acre ft and net volume 96320.13acre ft of reservoir sand (Table 1).

### **OJ-01 Well**

The entire studied depth of OJ-01 well is from -7042.86ft (-2146.66m) to -9306.00ft (-2836.47m) *tvdss*. Four potential sand reservoirs are observed within this depth. The first, Sand\_A which occurs within -7042.86ft (-2146.66m) to -7134.62ft (-2174.63m) *tvdss* with a thickness of 91.76ft (27.97m) contains oil. It shows similarity with Sand\_C (-9154.93ft (-2790.42m) to -9211.92ft (-2807.79m)) and Sand\_D (-9243.89ft (-2817.54m) to -9306.00ft (-2836.47m)) with thicknesses of 56.99ft (17.37m) and 62.11ft (18.93m) respectively except Sand\_B (-7709.19ft (-2349.76m) to -8045.92ft (-2452.40m)) with thickness of 336.73ft (102.64m) contains oil and water at -7877.56ft (-2401.08m). The petrophysical parameters calculated within this well are good with porosity ranging from 26 - 37%. Also, the values of water saturation, Sw, further indicate the presence of hydrocarbon and a gradual reduction in permeability is observed perhaps due to compaction caused by overburden. The total resistivity and water

saturation value of Sand\_B is lower and higher than the others due to the presence of water in the reservoir. The cross plots of log-K/ of the well indicate the sands are medium-fine grained. The volume of shale also ranges from 0.013 to 0.041 and these Vsh values are within the limit that could not affect the value of water saturation [25]. This

suggests that reservoirs present in OJ-01 well are relatively clean (Tables 1, 2, Figs. 8 and 9).

The total amount of about 5.21MMbbl is recovered from the Stock Tank Oil In Place (STOIP) of about 65.964MMbbl with a low recovery factor of 13.5%. This is attributed to lack of gas drive and hydrocarbon viscosity.

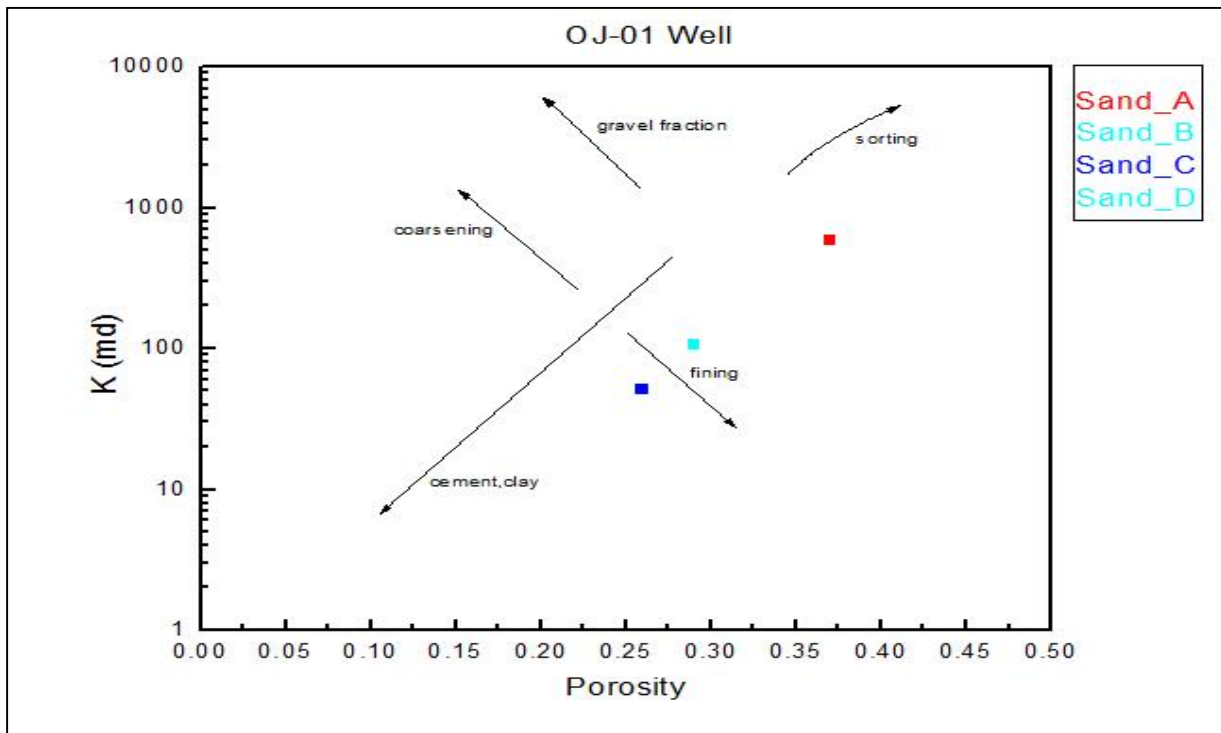


Fig. 8: Permeability-positivity plots for OJ-01 well (modified after Nelson 1994).

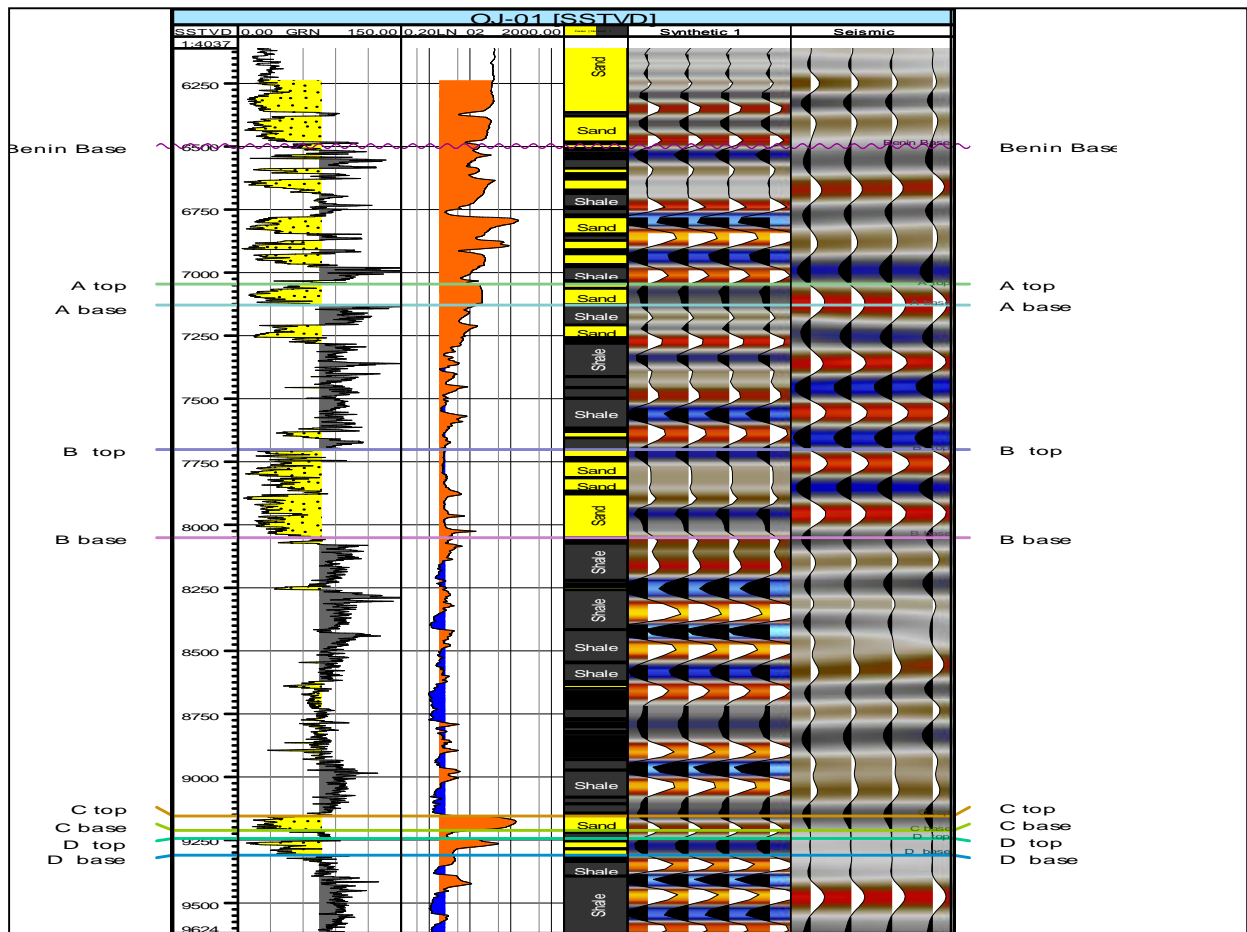


Fig. 9: The OJ-01 well log showing the potential reservoir sands.

**Table 1: Petrophysical Parameters Results of OJ-Field**

Well no	Well	MD, (ft)/(m)	TopMD, (ft)/(m)	Base MD, (ft)/(m)	TVDSS, (ft)/(m)	Gross Interval	Gross Res	Net Res	Net Pay	N/G	Phi	Phi E	Sw	Vsh	BVW	K (md)	Swir	Contact	Fluid type
<b>Sand A</b>																			
1	OJ-01	7209.84 (2197.56)	7163.96 (2183.58)	7255.72 (2211.54)	-7088.74 (-2160.65)	91.76	81.49	82.99	79.85	0.87	0.37	0.37	0.14	0.013	0.052	587.27	0.054	ODT	Oil
2	OJ-02	7232.63 (2204.51)	7196.79 (2193.58)	7268.46 (2215.43)	-7104.53 (-2165.49)	71.67	67.08	48.67	67.08	0.94	0.38	0.36	0.20	0.060	0.072	540.40	0.053	ODT	Oil
3	OJ-03	7265.28 (2214.46)	7223.59 (2201.75)	7306.97 (2227.16)	-7143.18 (-2177.24)	83.38	89.36	87.77	78.22	0.94	0.32	0.32	0.18	0.011	0.058	227.78	0.063	ODT	Oil
4	OJ-04	6854.83 (2089.35)	6818.25 (2078.20)	6891.40 (2100.50)	-6723.93 (-2049.45)	73.15	65.57	52.33	56.77	0.78	0.26	0.25	0.29	0.027	0.073	51.46	0.077	ODT	Oil
<b>Sand B</b>																			
1	OJ-01	7998.66 (2437.99)	7830.29 (2386.67)	8167.02 (2489.31)	-7877.56 (-2401.08)	336.73	167.69	348	22.40	0.07	0.29	0.28	0.31	0.042	0.087	105.52	0.069	OWC	Oil, Water
2	OJ-02	7937.34 (2419.30)	7774.52 (2369.67)	8100.16 (2468.93)	-7809.34 (-2380.29)	325.64	312.98	189.30	67.08	0.21	0.29	0.25	0.69	0.122	0.173	64.09	0.069	WET	Water
3	OJ-03	7916.30 (2412.89)	7830.29 (2386.67)	8002.30 (2439.10)	-7794.20 (-2375.67)	172.01	167.69	151.80	0	-	0.31	0.29	0.68	0.051	0.197	134.76	0.065	WET	Water
4	OJ-04	7312.02 (2228.70)	7168.84 (2185.06)	7455.19 (2272.34)	-7181.12 (-2188.81)	286.35	281.28	268.20	254.90	0.89	0.33	0.31	0.23	0.047	0.071	21.29	0.061	ODT	Oil
<b>Sand C</b>																			
1	OJ-01	9304.53 (2836.02)	9276.03 (2827.33)	9333.02 (2844.70)	-9183.43 (-2799.11)	56.99	50.93	50.93	50.93	0.89	0.26	0.25	0.08	0.041	0.020	51.46	0.077	ODT	Oil
2	OJ-02	9331.15 (2844.14)	9292.90 (2832.48)	9369.40 (2855.79)	-9203.15 (-2805.12)	76.50	75.03	17.52	67.08	0.88	0.49	0.38	0.40	0.216	0.152	1145.56	0.041	OWC	Oil, Water
3	OJ-03	9248.65 (2818.99)	9212.30 (2807.91)	9284.99 (2830.07)	-9126.55 (-2781.77)	72.69	70.26	60.71	0	-	0.37	0.36	0.51	0.040	0.184	520.57	0.054	WET	Water
4	OJ-04	8474.27 (2582.96)	8428.66 (2569.06)	8519.87 (2596.86)	-8343.37 (-2543.06)	91.21	88.92	70.03	0	-	0.24	0.23	0.59	0.056	0.136	29.96	0.084	WET	Water
<b>Sand D</b>																			
1	OJ-01	9396.05 (2863.92)	9364.99 (2854.45)	9427.10 (2873.38)	-9274.95 (-2827.01)	62.11	65.49	63.89	38.31	0.62	0.29	0.28	0.12	0.041	0.034	105.52	0.069	ODT	Oil
2	OJ-02	9806.46 (2989.01)	9758.79 (2974.48)	9854.12 (3003.54)	-9678.46 (-2950)	95.33	95.73	46.27	75.04	0.79	0.44	0.35	0.53	0.195	0.186	631.76	0.046	WET	Water
3	OJ-03	9366.06 (2854.78)	9318.26 (2840.21)	9413.85 (2869.34)	-9243.96 (-2817.56)	95.59	94.47	83.10	9.56	0.10	0.34	0.33	0.48	0.032	0.158	297.37	0.059	OWC	Oil, Water
4	OJ-04	8602.73 (2622.11)	8550.56 (2606.21)	8654.89 (2638.01)	-8471.43 (-2582.21)	104.33	99.14	88.95	65.62	0.63	0.23	0.22	0.08	0.051	0.018	2297	0.087	GOC	Oil, Gas

**Table 2: Reserve Calculation Results of OJ-Field**

Well no	Well	Phi	Sw	(1 - Sw)	Net Pay	Gross Int. (ft)	N/G	Net Res. (ft)	Gross Res. (ft)	Area (oil) (acre)	Area (gas) (acre)	Gross Vol. (acre ft)	Net Vol. (acre ft)	RF (%)	OIIP (stb)	STOIP (MMbbl)	GIP, (MMcf)	N = (RF x STOIP) (MMbbl)
Sand_A																		
1	OJ-01	0.37	0.14	0.86	79.85	91.76	0.87	82.99	81.49	211	-	17194.39	14959.12	9.1	4759.992	30.773347	-	2.800375
2	OJ-02	0.38	0.20	0.80	67.08	71.67	0.94	48.67	67.08	89	-	5970.12	5611.91	15.5	1706.021	11.029429	-	1.709561
3	OJ-03	0.32	0.18	0.82	78.22	83.38	0.94	87.77	89.36	89	-	7953.04	7475.86	12.5	1961.665	12.682164	-	1.585271
4	OJ-04	0.26	0.29	0.71	56.77	73.15	0.78	52.33	65.57	26	-	1704.82	1329.76	23.1	245.4736	1.586987	-	0.366594
Sand_B																		
1	OJ-01	0.29	0.31	0.69	22.40	336.73	0.07	348	167.69	470	-	78814.3	5517.00	25.9	1103.952	7.137049	-	1.848496
2	OJ-02	0.29	0.69	0.31	67.08	325.64	0.21	189.30	312.98	-	-	-	-	-	-	-	-	-
3	OJ-03	0.31	0.68	0.32	0	172.01	-	151.80	167.69	-	-	-	-	-	-	-	-	-
4	OJ-04	0.33	0.23	0.77	254.90	286.35	0.89	268.20	281.28	46	-	12938.88	11515.60	18	2926.115	18.917332	-	3.40512
Sand_C																		
1	OJ-01	0.26	0.08	0.92	50.93	56.99	0.89	50.93	50.93	254	-	12936.22	11513.24	-	2753.966	17.804390	-	-
2	OJ-02	0.49	0.40	0.60	67.08	76.50	0.88	17.52	75.03	254	-	19057.62	16770.71	37.4	4930.587	31.876248	-	11.92172
3	OJ-03	0.37	0.51	0.49	0	72.69	-	60.71	70.26	-	-	-	-	-	-	-	-	-
4	OJ-04	0.24	0.59	0.41	0	91.21	-	70.03	88.92	-	-	-	-	-	-	-	-	-
Sand_D																		
1	OJ-01	0.29	0.12	0.88	38.31	62.11	0.62	63.89	65.49	153	-	10019.97	6212.38	5.5	1585.4	10.249609	-	0.563728
2	OJ-02	0.44	0.53	0.47	75.04	95.33	0.79	46.27	95.73	-	-	-	-	-	-	-	-	-
3	OJ-03	0.34	0.48	0.52	9.56	95.59	0.10	83.10	94.47	78	-	7368.66	736.87	44.7	130.2779	0.8422467	-	0.376484
4	OJ-04	0.23	0.08	0.92	65.62	104.33	0.63	88.95	99.14	235	112	23297.9	14677.68	-	3105.796	20.078974	112.740411	-
										<b>Total</b>		<b>197255.92</b>	<b>96320.13</b>		<b>25209.25</b>	<b>162.9778</b>	<b>112.740411</b>	<b>24.57735</b>

**OJ-02 Well**

The total depth of investigation of OJ-02 well occurred from -7068ft (-2154.33m) to -9726.12ft (-2964.52m) *tvds* with shale occurring predominantly (Fig. 10). Sand\_A which contain oil ranges from -7068.79ft (-2154.57m) to -7184.87ft (-2189.95m) *tvds* and has a thickness of 71.67ft (21.85m). The next potential reservoir sand has a thickness of 76.50ft (23.32m) and it occurs between -9164.90ft (-2793.46m) to -9241.40ft (-2816.78m) *tvds*. It has fluid content of oil and water with OWC at -9203.15ft (-2805.12m) *tvds*. Sand\_B (-7646.52ft (-2330.66m) to -7972.16ft (-2429.91m) *tvds*) and Sand\_D (-9630.79ft (-2935.47m) to -9726.12ft (-2964.52m) *tvds*) reservoirs are wet and they have thicknesses of 325.64ft (99.26m) and 95.33ft (29.06m) respectively. The result reveals that the water saturation of Sand\_B and Sand\_D are above 50% which

suggest that the reservoirs are mainly water bearing. The porosity of Sand\_A and Sand\_C are greater than 10% and in connection with their water saturation shows that they are good potential hydrocarbon reservoir. The total resistivity value of Sand\_C is lower than that of Sand\_A due to the presence of water in the reservoir. Though, the values of volume of shale and permeability indicate that OJ-02 well has good potential reservoir sands while the bulk volume water and the cross plots of log-K/ of the well reflect that the potential reservoir sands are fine grained sand (Tables 1, 2, Figs. 9 and 10).

OJ-02 well stock tank oil in place (STOIP) is about 42.91MMbbl. With recovery factor of 26.5%, only 13.63MMbbl is recovered from the well and this occur as a result of viscosity of the hydrocarbon and the gas drive.

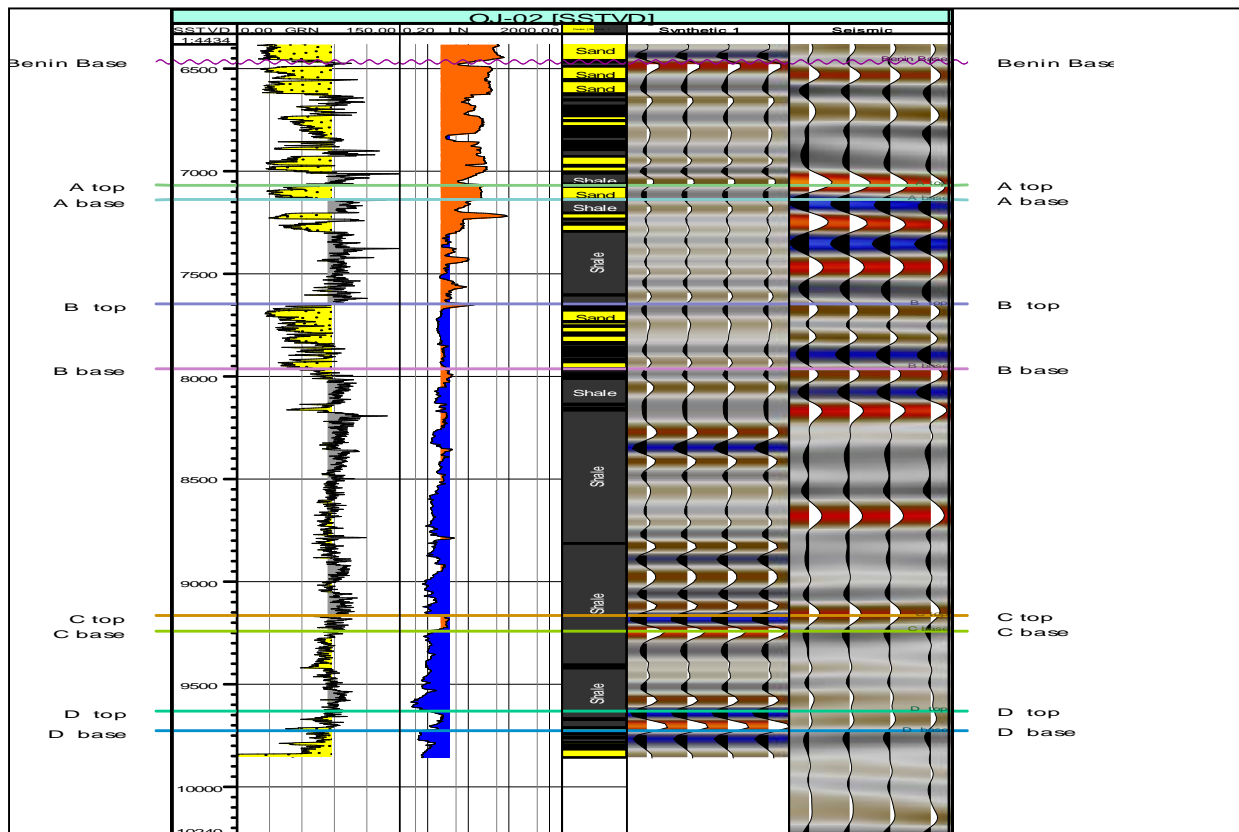


Fig. 10: The OJ-02 well log showing the potential reservoir sands.

**OJ-03 Well**

The four potential reservoir sands are also observed in this well and appear to be lateral continuities of the sands in OJ-02 well. Its depth of investigation ranges from -7101.49ft (-2164.53m) to -9291.75ft (-2832.13m) *tvds*. The Sand\_A is within -7101.49ft (-2164.53m) to -7184.87ft (-2189.95m) *tvds* with a thickness of 83.38ft (25.41m) hydrocarbon while Sand\_B (-7708.19ft (-2349.46m) to -7880.20ft (-2401.89m) *tvds*) and Sand\_C (-9090.20ft (-2770.69m) to -9162.89ft (-2792.85m)) are wet and they have thicknesses of 172.01ft (52.43m) and 72.69ft (22.16m) respectively. Sand\_D is the second hydrocarbon zone in the well. It occurs between -9196.16ft (-2802.99m) to -9291.75ft (-2832.13m) *tvds* and has a thickness of 95.59ft (29.14m).

In Table 1 below, the water saturation of Sand\_B and Sand\_C are above 50% which suggest that the reservoirs are mainly water

bearing while its below 50% in Sand\_A and Sand\_D reservoirs indicating hydrocarbon bearing zone. The total resistivity values of Sands\_B, C and D are lower than that of Sand\_A which also indicates the presence of water in the reservoirs. Though, Sand\_D total resistivity value is higher than the water bearing sands. The volume of shale ranges from 0.011 – 0.051 which indicates that the reservoir sands are clean. The values of porosity and permeability are also good enough to permit free flow of fluid while the cross plots of log-K/ and bulk volume of water that ranges from 0.058 – 0.197 suggest that the sands are medium-fine grained (Tables 1, 2, Figs. 11 and 12). With recovery factor of about 28.6%, only 1.96MMbbl is recovered out of stock tank oil in place (STOIP) of about 13.52MMbbl of the well. This can be attributed to lack of gas drive and viscosity.

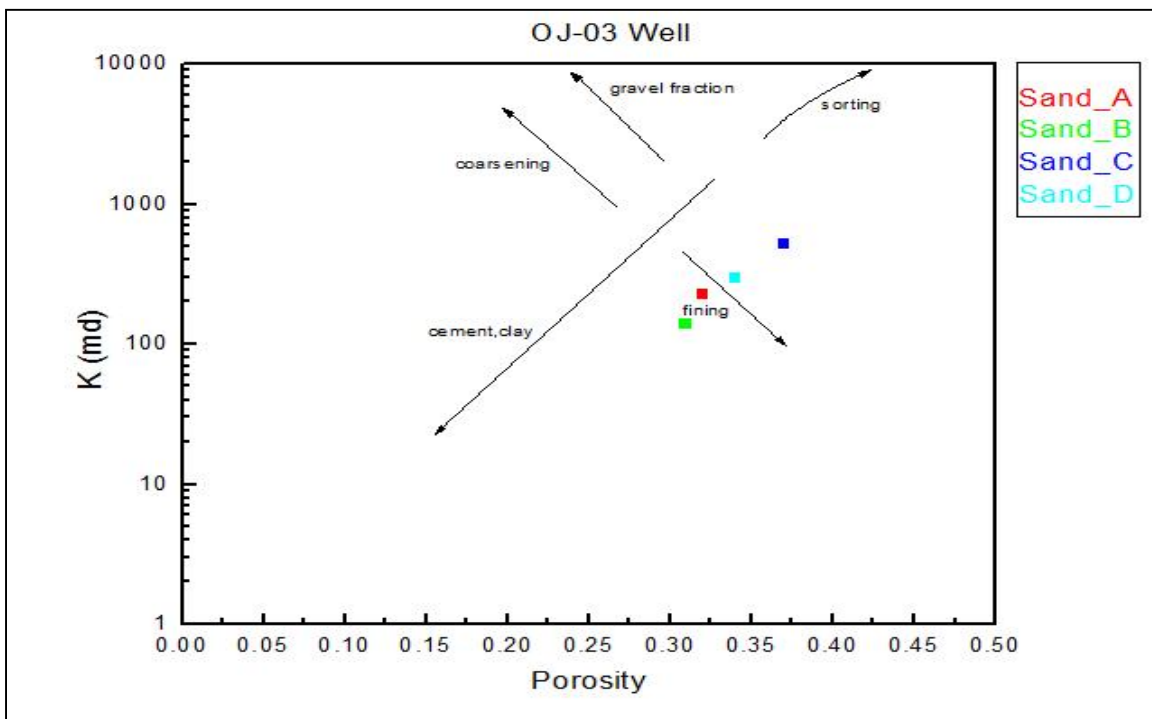


**Fig. 11:** Permeability-porosity plots for OJ-03 well (modified after Nelson 1994).

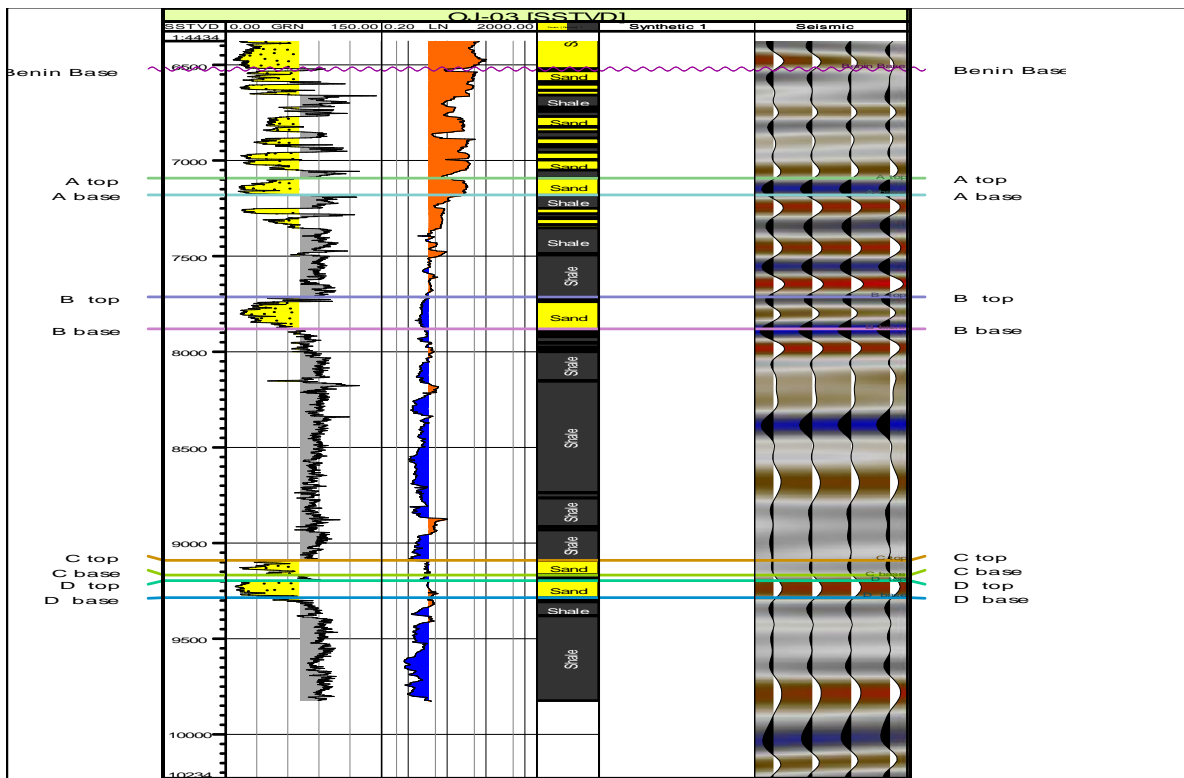


Fig. 12: The OJ-03 well log showing the potential reservoir sands.

**OJ-04 Well**

This well occurs in the northwestern part of OJ-field and shows the occurrence of four potential reservoir sands within the interval studied, -6687.35ft (-2038.30m) to -8523.99ft (-2598.11m) *tvds*s. The first potential sand, Sand\_A occurs within the depth range of -6687.35ft (-2038.30m) to -6760.50ft (-2060.60m) *tvds*s. It shows similarity with other Sands\_A in its fluid content and its reservoir thickness is 73.15ft (22.30m). Sand\_B also has the same fluid content similar to the first potential sand and it occurs within -7037.94ft (-2145.16m) to - 7324.29ft (-2232.44m) *tvds*s with a thickness of 286.35ft (87.28m). Sand\_C indicates a zone of water bearing reservoir with a thickness of 91.21ft (27.80m) and occurs within the depth -8297.76ft (-2529.16m) to -8388.97ft (-2556.96m). The fourth reservoir, Sand\_D occurs within -8419.66ft (-2566.31m) to -8523.99ft (-2598.11m) with a thickness of 104.33ft (31.80m). It has fluid content of oil and gas with GOC at -8471.83ft (-2582.21m). From Table 2, it is shown that the total

resistivity value of Sand\_C is the lowest out of all the reservoir sands and with focus on its water saturation (>50%) suggests that Sand\_C is mainly water bearing reservoir. Also, Sand\_D has the highest total resistivity value, and the negative crossing of the density log and neutron log signature at -8420ft (-2566.42m) to -8440ft (-2572.51m) *tvds*s suggests that it is a gas zone and the thickness of the gas is 20ft (6.10m). Sand\_A and Sand\_B water saturation (< 50%) shows that the reservoirs are oil bearing zone. The porosity, permeability and volume of shale values also reveal that the well has good potential reservoir sand which is good enough to allow free flow of fluid. The bulk volume of water and the cross plots of log-K/ indicate the potential sands as medium-fine grained (Tables 1, 2, Figs. 13 and 14). The stock tank oil in place (STOIP) of well OJ-04 is about 40.6 and 3.77MMbbl s recovered with a recovery factor of about 20.6%. Also, the gas in place (GIP) of the well is about 112.74MMcf and the low recovery factor can be attributed to the viscosity of the oil.

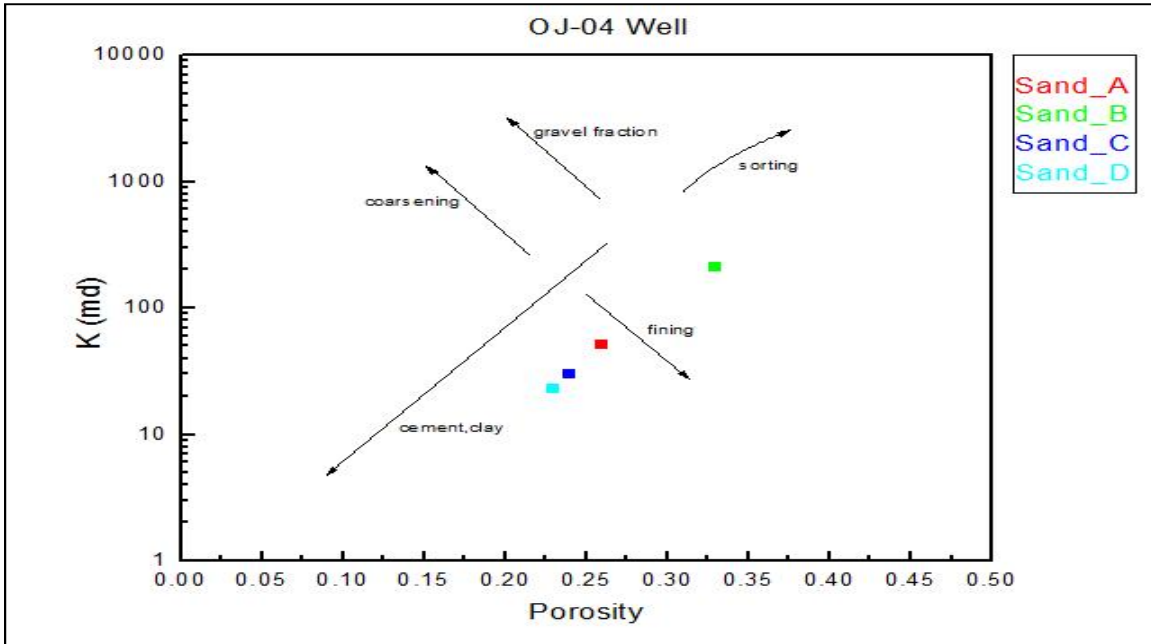


Fig. 13: Permeability-porosity plots for OJ-04 well (modified after Nelson 1994).

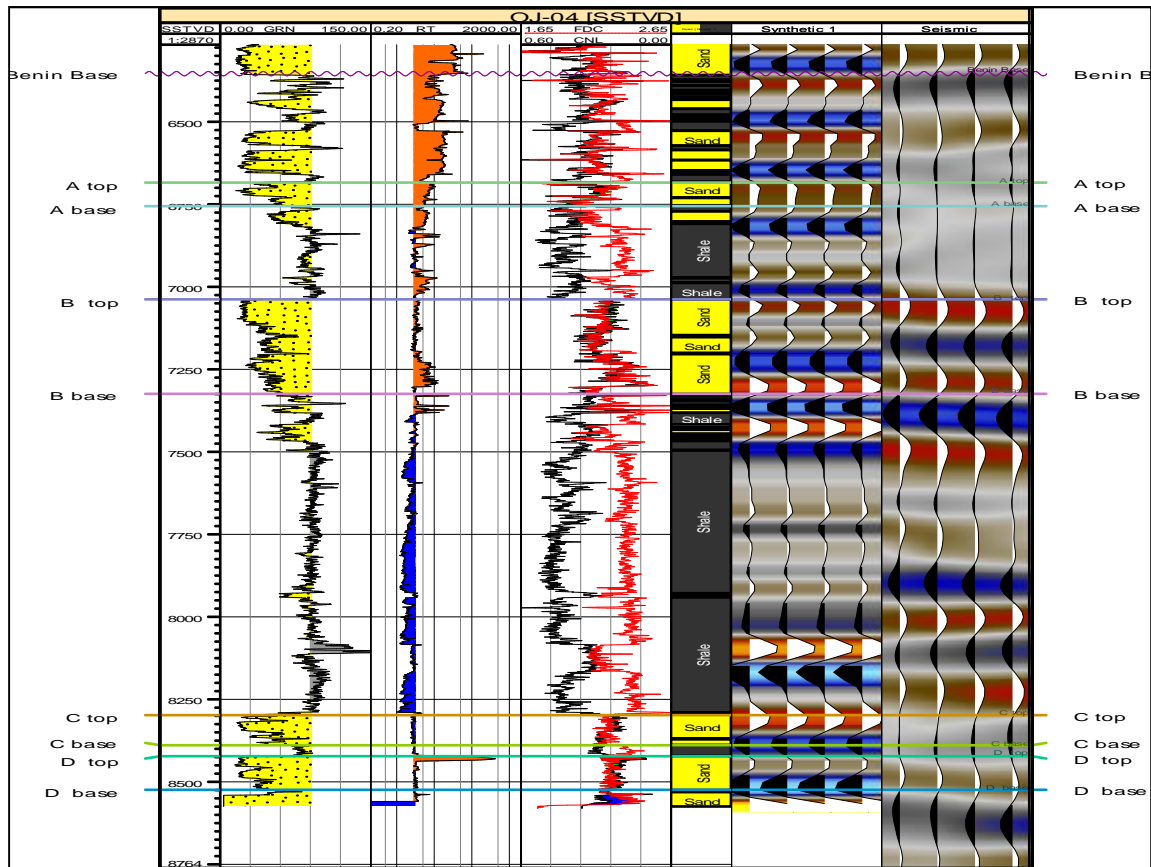


Fig. 14: The OJ-04 well log showing the potential reservoir sands.

### Seismic Interpretation

The time migrated and processed seismic data reflect the true amplitude of events in the field. Overall appearance reflection patterns are generally continuous except in areas with faults and marine shales. Based on their absorption coefficient, negative amplitude in the section (blue) represents shale, whereas the positive amplitude (red) represents sandstone or sandy shale formations (Fig. 13). Changes in the behaviour of the amplitude reflect the exact subsurface condition; thus, the structural and stratigraphic nature of the field was resolved. The fairly continuous high amplitude reflections from 1600 to 2600ms of two-way travel time suggest the sand-shale sequence of high energy environments of Agbada Formation. Below this time, reflection gradually becomes chaotic and discontinuous, suggesting the presence of marine shale of Akata Formation (Fig. 15). From the seismic section it is evident that the field is faulted with marked synthetic and antithetic faults (F<sub>1</sub> and F<sub>5</sub>). Only normal faults are associated

with the field, two of which are growth faults cutting through the field from west to east. The two growth faults (F<sub>1</sub> and F<sub>2</sub>) along with Faults F<sub>3</sub> and F<sub>4</sub> dip southeast and trend northwest, whereas Faults F<sub>5</sub> and F<sub>6</sub> trend northeast and dip southwest. Faults F<sub>5</sub> and F<sub>6</sub> are antithetic, associated with coastal regions of Niger Delta [1]. The presence of only normal faults in the field indicates an extensional deformational phase during subsidence and uplift associated with instability of the overpressured Late Cretaceous shale.

These faults assisted in formation of roll-over anticline structures and trapping of the migrating hydrocarbon from lower transgressive shale. The faults divided the field into four major faults blocks at each reservoir level. The depth structure maps show that the wells are on the fault F<sub>1</sub> downthrown side but up thrown side of F<sub>2</sub>. The migration and trapping of hydrocarbons were facilitated by the presence of these faults assisted by shale bodies to form structural closures (Fig. 16).

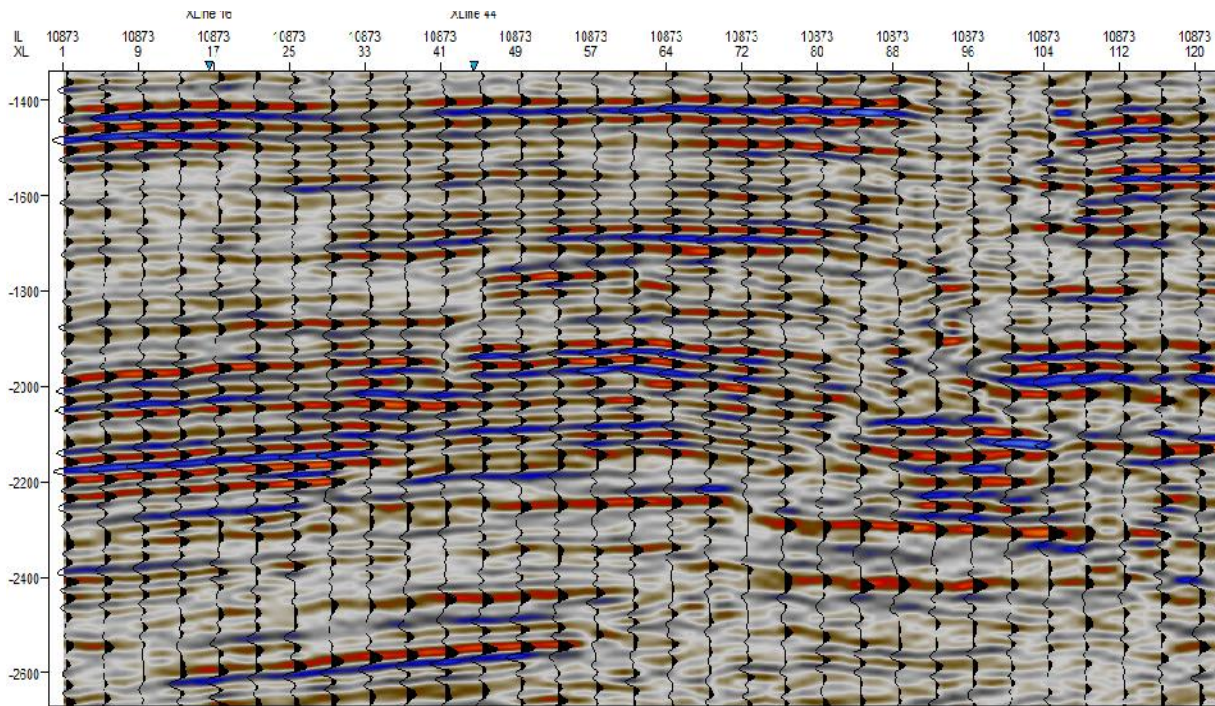
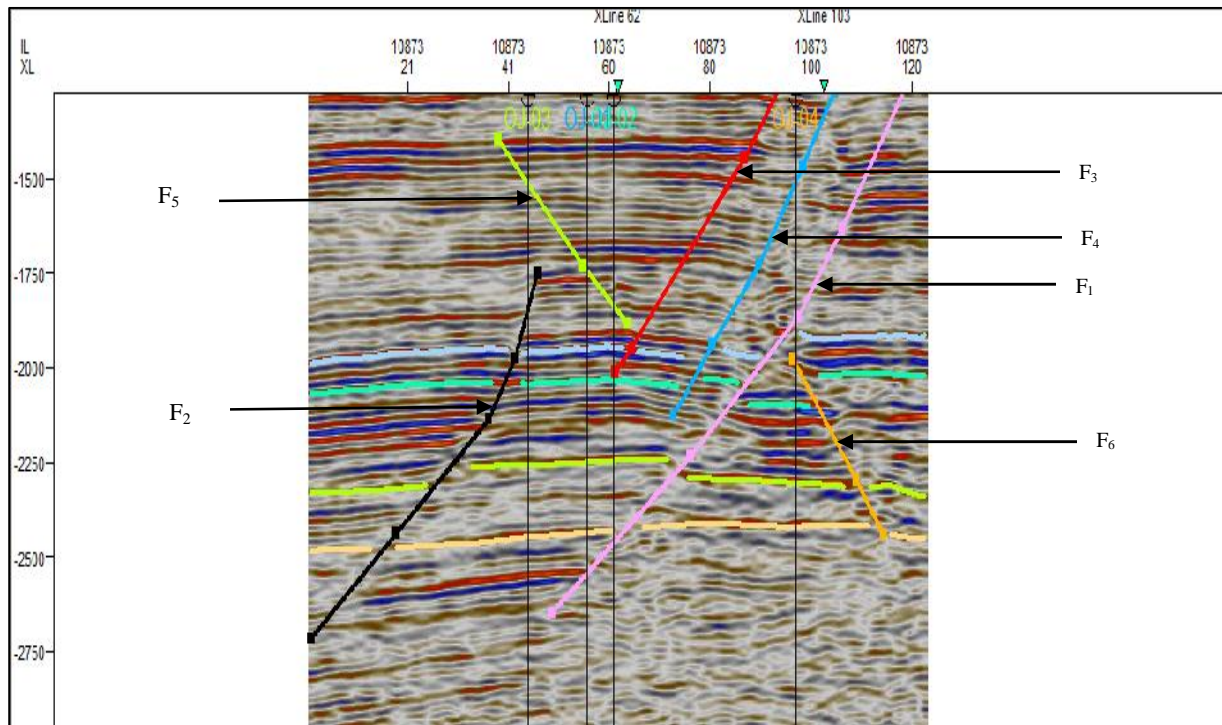


Fig. 15: Seismic in-line 10873 showing the positive (sandstone) and negative (shale) amplitudes.



**Fig. 16:** Seismic in-line 10873 showing mapped reservoirs and fault system.

## Reservoirs Potential

### *Reservoir 1: Sand\_A*

Sand\_A is the first and most prolific in hydrocarbon-bearing horizon occurring at -7088.74ft (-2160.65m), -7104.63ft (-2165.49m), -7143.18ft (-2177.24m) and -6723.93ft (-2049.45m) for OJ-01, OJ-02, OJ-03 and OJ-04 respectively. The reservoir has average porosity value of 33.3% with volume of shale content ranging from 0.011 to 0.060. The water saturation ranges from 14% to 29% and the plots of log-Rt/Sw indicate the contact is oil-down-to (ODT) in all the wells present and this reveals that the reservoir fluid is mainly oil. Sand\_A's top depth structure map has maximum and

minimum contour values of -6720ft (-2048.26m) to -8560ft (-2609.09m) and -7120ft (-2170.18m) to -8960ft (-2731.01m) for its base respectively and its gross thickness ranges from 0 – 350ft (0 – 106.68m). It has oil initially in place (OIIP) of about 8673.152stb and this amount has a surface equivalence (STOIP) of about 56.07MMbbl of oil (Tables 1, 2, Figs. 17 and 18). With a recovery factor of about 15.05%, only 6.46MMbbl can be produced from the reservoir. The low recovery factor can be attributed to lack of gas drive, appreciable water drive and hydrocarbon viscosity since the recovery factor is dependent on the drive mechanism and viscosity [26].

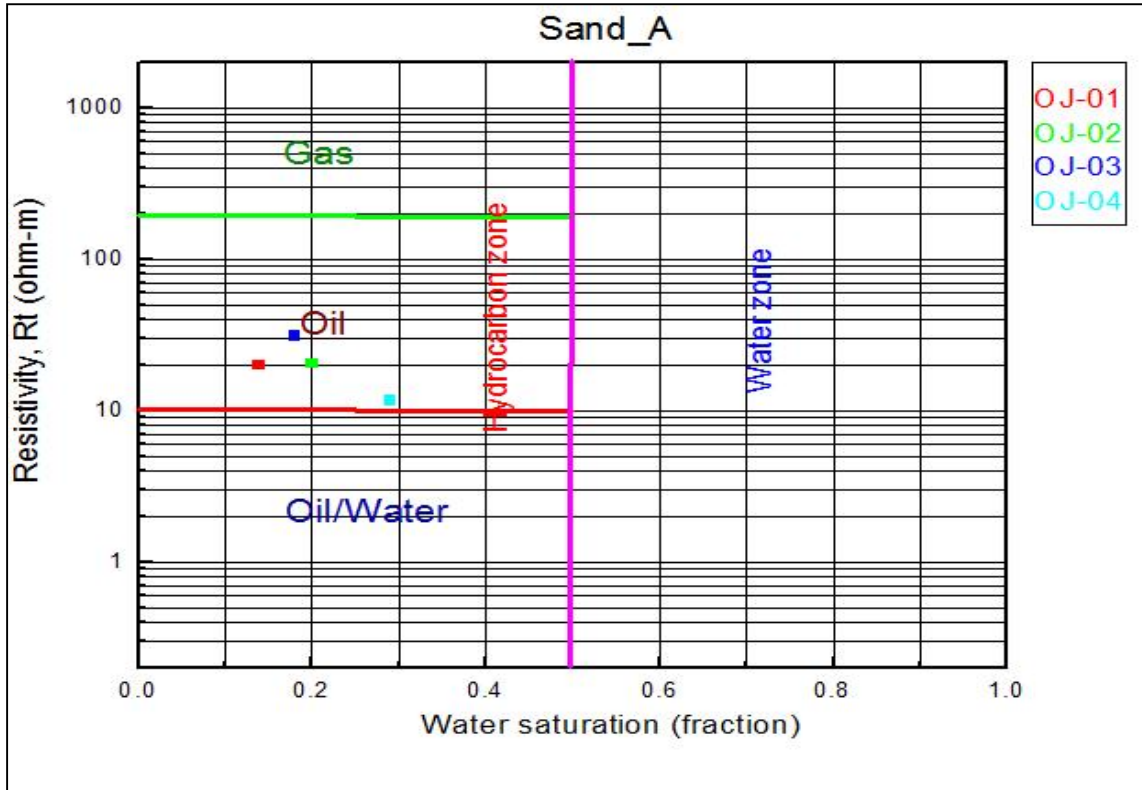


Fig. 17: Plot of water saturation against resistivity of Sand\_A.

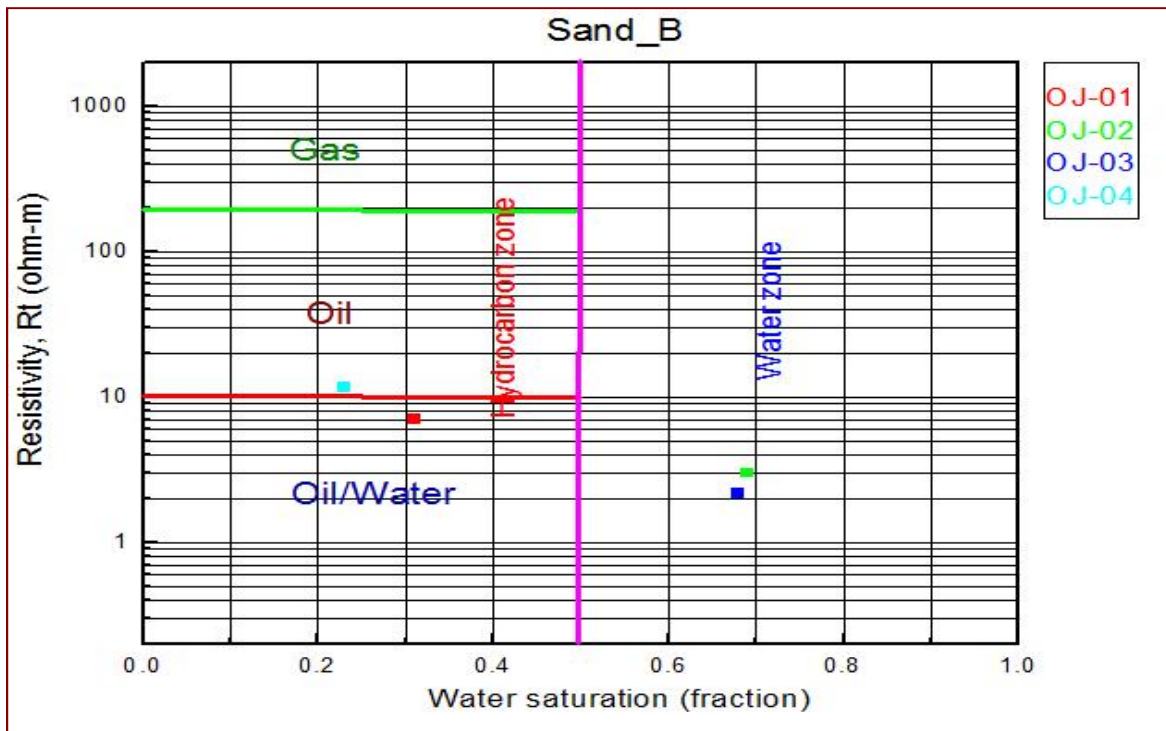


Fig. 18: Sand\_A top (A) and base (B) depth structural maps.

### ***Reservoir 2: Sand\_B***

Sand\_B is the second reservoir, least prolific in oil but with the largest prospect of the four depicted reservoirs. This sandstone reservoir unit occurred at a subsea depth of -7181.12ft (-2188.81m) to -7877.56ft (-2401.08m) and it is sealed above and below by a thick sequence of shale. Its altitude and lowest point are shown by maximum and minimum contour values of -7050ft (-2148.84m) to -8050ft (-2453.64m) for Sand\_B top and -7500ft (-2286m) to -8500ft (-2590.80m) for its base. The average porosity value of the reservoir is 30.5% with volume of shale content ranging from 0.042 to 0.122. The reservoir gross thickness ranges from 90 - 300ft, a net thickness of at least 151ft

(46.02m) in all the wells and a net pay of about 22ft (6.71m) for OJ-01 and 255ft (77.72m) for OJ-04. OJ-02 and OJ-03 contain only water, as shown by their water of saturation values of 69 and 68% respectively (Tables 1, 2, Figs. 19 and 20). The wetness results from fault displacement below the oil water contact level of the hydrocarbon-bearing sands. The reservoir produces oil in wells OJ-01 and OJ-04 with oil initially in place (OIIP) of about 4030.067stb and STOIP of about 26.05MMbbl. The recovery factor of about 22% recovers 5.25MMbbl which shows that the low recovery can be caused by the hydrocarbon viscosity and drive mechanism (gas drive) [26].

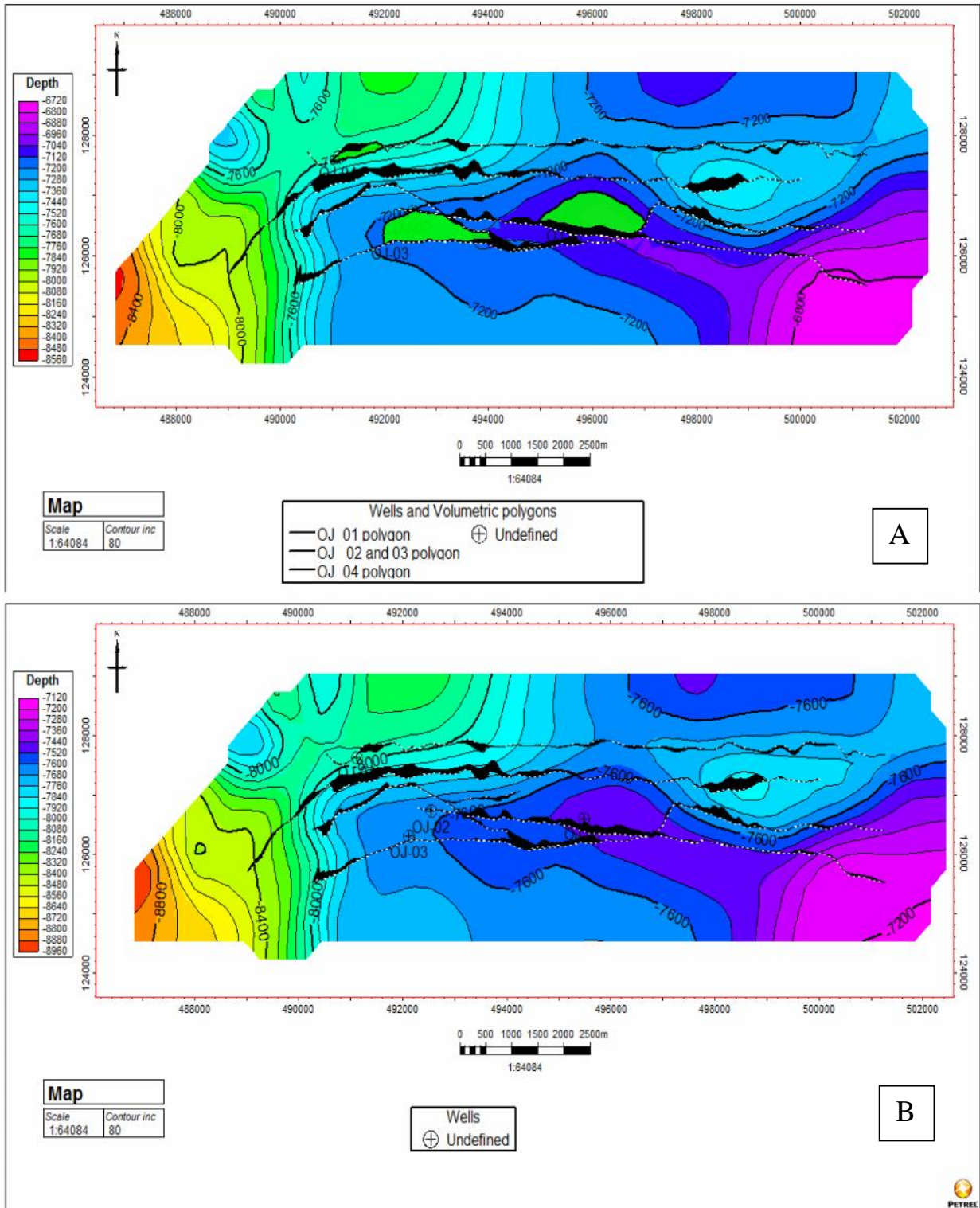


Fig. 19: Plot of water saturation against resistivity of Sand\_B (modified after Schlumberger 1998).

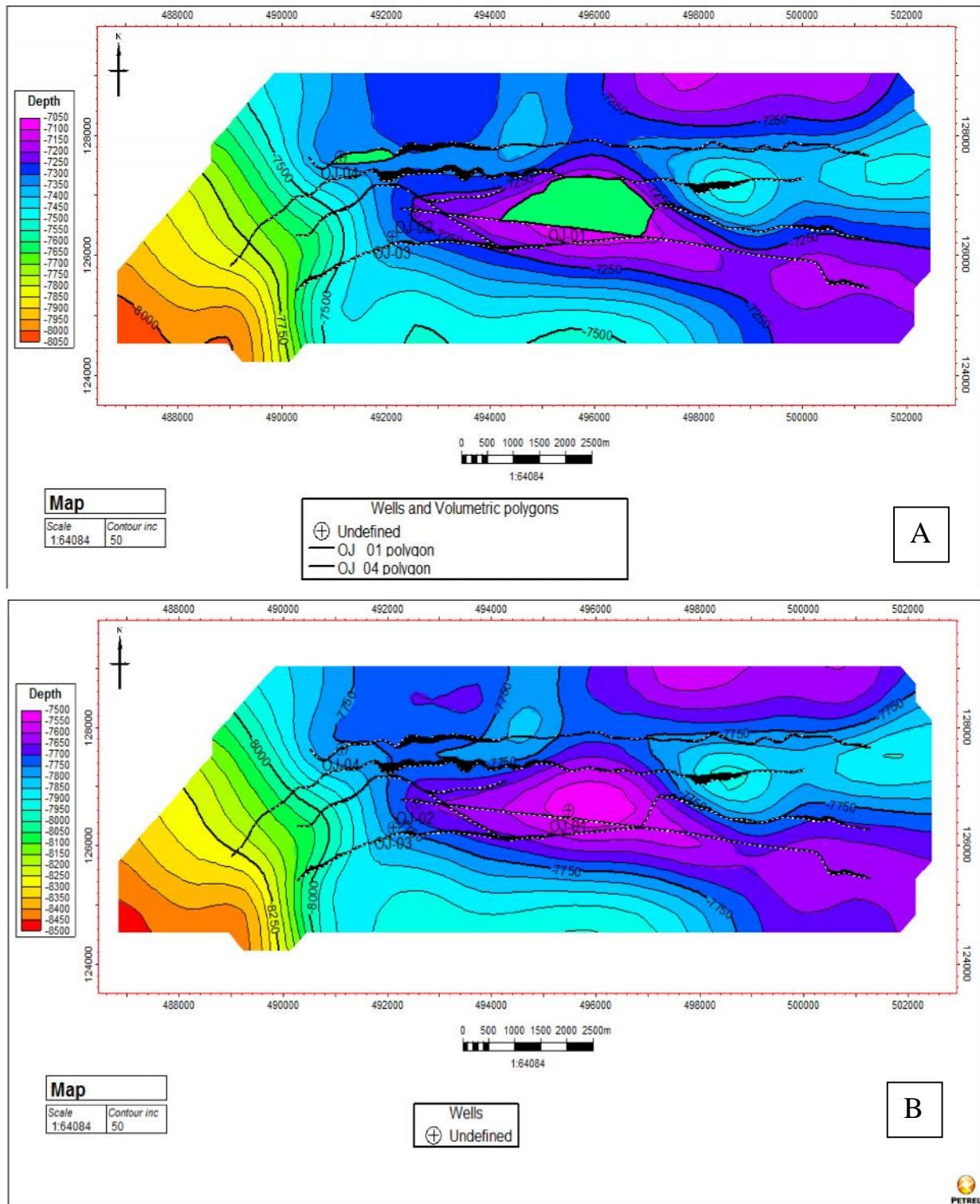
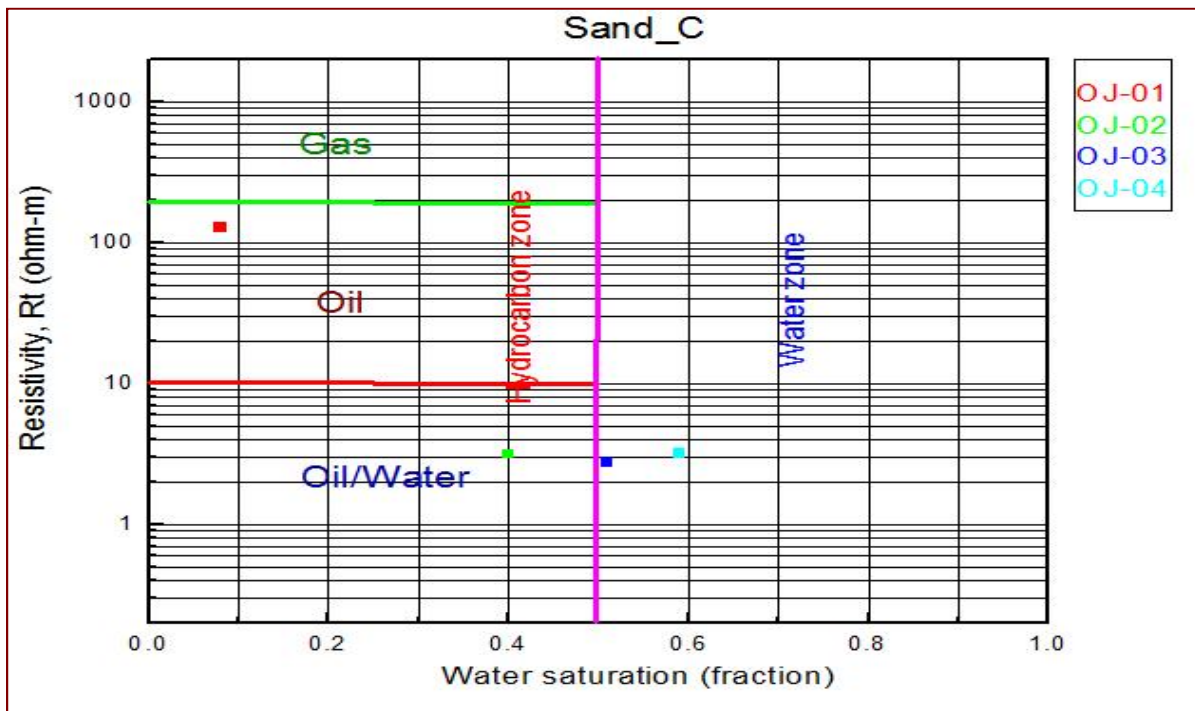


Fig. 20: Sand\_B top (A) and base (B) depth structural maps.

**Reservoir 3: Sand\_C**

Sand\_C is the second most prolific hydrocarbon-bearing horizon of the four reservoirs analyzed in this field (Fig. 21). It is located at subsea measurements of -9183.43ft (-2799.11m), -9203.15ft (-2805.12m), -9126.55ft (-2781.77m), and -8343.37ft (-2543.06m) for OJ-01, OJ-02, OJ-03 and OJ-04 respectively. The depth structure map of this sandstone reservoir unit has maximum and minimum contour values -7800ft

(-2377.44m) to -9000ft (-2743.20m) (top) and -8200ft (-2499.36m) to -9400ft (-2865.12m) (base) respectively. The reservoir has average porosity of 34% with volume of shale content ranges from 0.040 to 0.216 and also its gross thickness ranges from 90 – 360ft (27.43 - 109.73m). OJ-03 and OJ-04 wells contain water shown by their water of saturation values which are above 50% (51 and 59% respectively) while OJ-01 contains only oil but OJ-02 fluids are oil and water (Fig. 22).



**Fig. 21:** Plot of water saturation against resistivity of Sand\_C (modified after Schlumberger 1998).

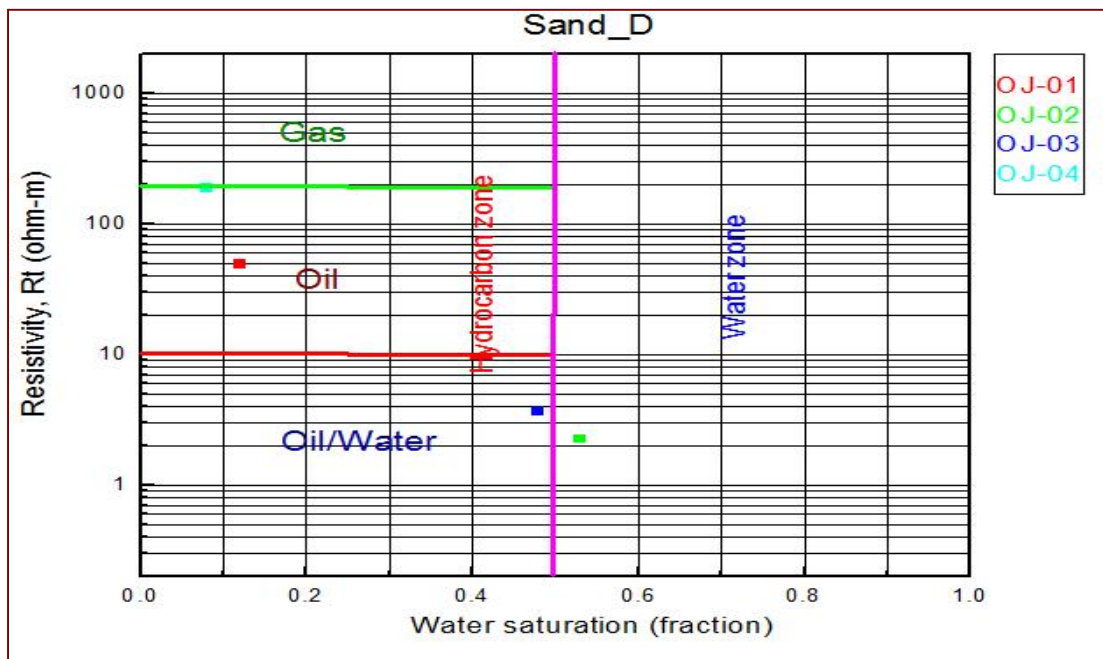


Fig. 22: Plot of water saturation against resistivity of Sand\_D (modified after Schlumberger 1998).

The oil initially in place (OIIP) of the Sand\_C reservoir is about 7684.553stb and the surface equivalence (STOIP) is about 49.68MMbbl. Only 11.92MMbbl can be produced from the reservoir with a recovery factor of about 37.4% and this is attributed to drive mechanism (lack of gas drive) and hydrocarbon viscosity since recovery factor is dependent on these factors (Tables 1 and 2) [26].

#### Reservoir 4: Sand\_D

Sand\_D is the last, deepest, and second least prolific in hydrocarbon. It occurs at a measured subsea depth of -8471.83ft (-2582.21m) to -9678.46ft (-2950m) with minimum net pay of 9.56ft (2.91m) for OJ-03, the thinnest of the hydrocarbon-bearing wells at this horizon. Faulting occurring at a level close to OJ-02 pushed its sand below the oil-water contact (OWC) of OJ-03, resulting in it being wet with a water saturation of 53%. The representative area of the individual reservoir bodies ranges from 78 to 235acre and the reservoir is bounded by a thick shale a thick shale sequence at the base and lesser amount at the top.

The depth structure map indicates the maximum and minimum contour values to be -7440ft (-2267.71m) to -9840ft (-2999.23m) for the top and -7840ft (-2389.63m) to -10240ft (-3121.15m) for the base. The reservoir gross thickness ranges from 180 – 450ft (54.86 - 137.16m) with average porosity value of 32.5% and the volume of shale content ranges from 0.032 to 0.195. The reservoir produced oil and gas, having oil-down to (ODC) for OJ-01 with water saturation of 12%, oil-water contact (OWC) for OJ-03 with water saturation of 48% and gas-oil contact (GOC) for OJ-04 with water saturation of 8% at -9274.95ft (-2827.01m), -9243.96ft (-2817.56m) and -8471.83ft (-2582.21m) respectively.

Sand\_D reservoir has oil initially in place (OIIP) of about 4821.474stb, stock tank oil in place (STOIP) of about 31.17MMbbl and also gas in place (GIP) of about 112.74MMcf. The reservoir produced about 0.94MMbbl with a recovery factor of 25.1% which shows that the low recovery factor can be caused by the hydrocarbon (oil) viscosity [26] (Tables 1, 2, Figs. 23 and 24).

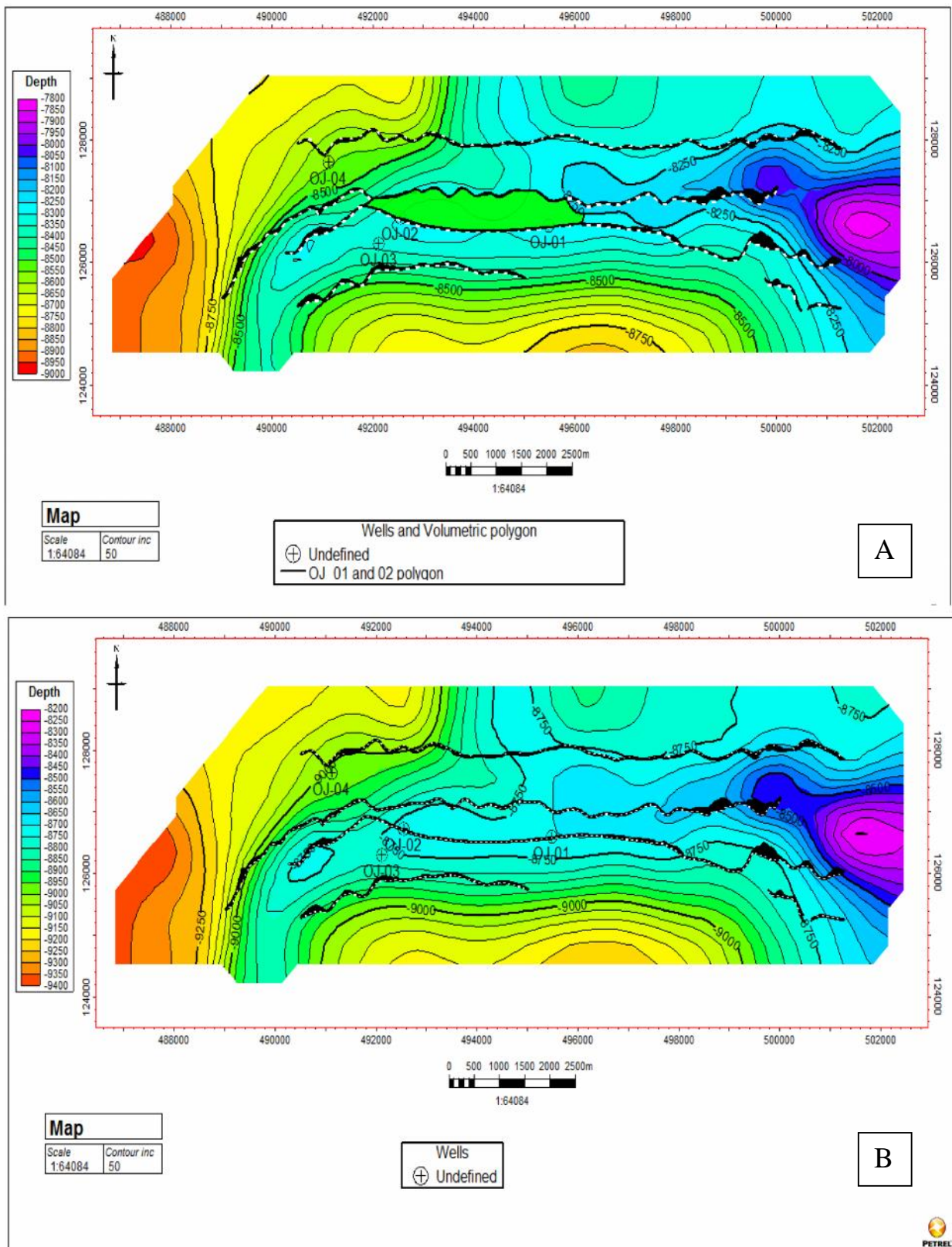


Fig. 23: Sand\_C top (A) and base (B) depth structural maps.

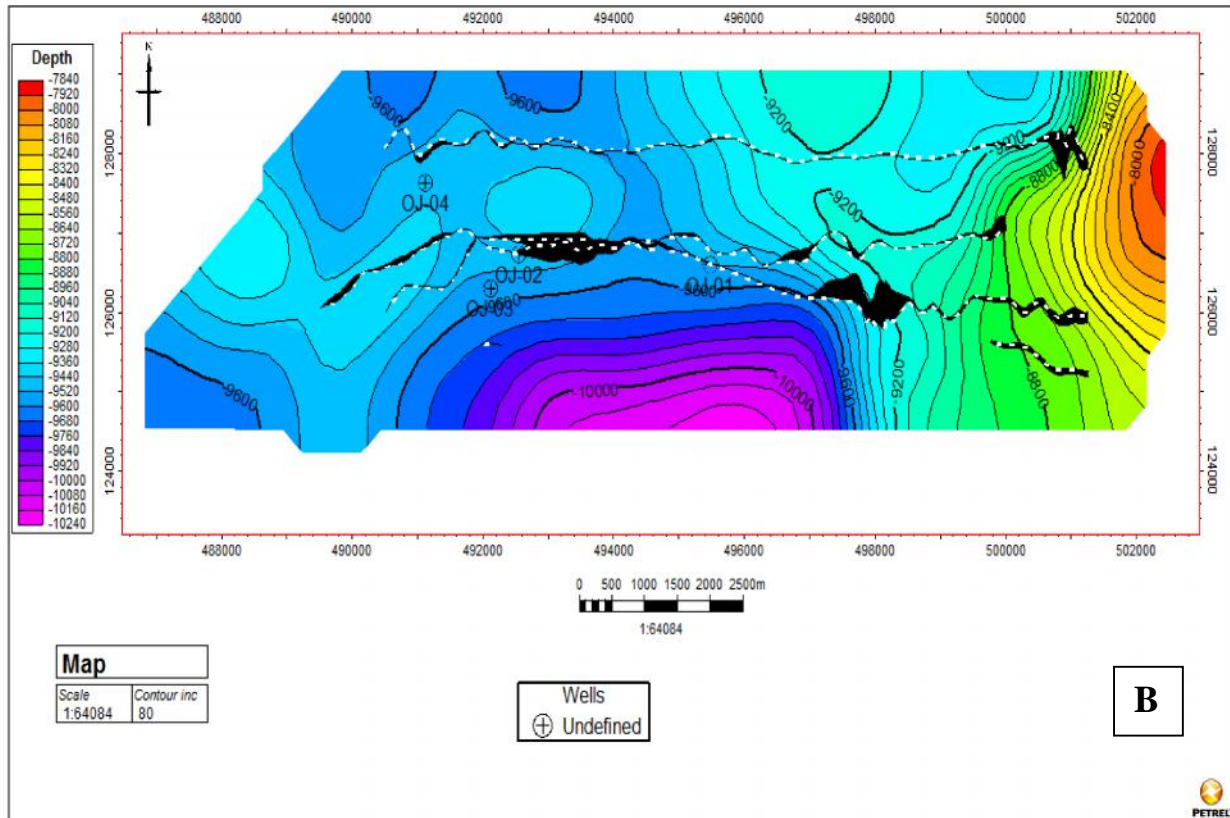
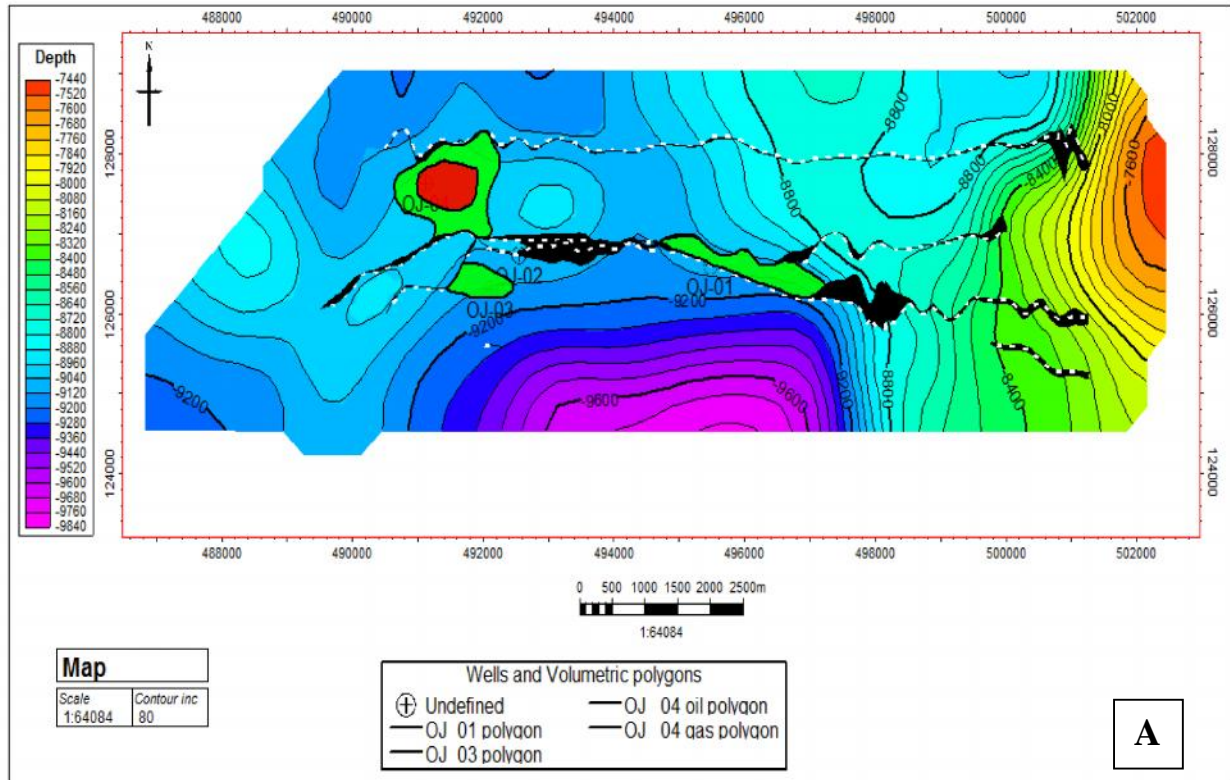


Fig. 24: Sand\_D top (A) and base (B) depth structural maps.

## Conclusion

This paper presents evaluation from four wells in 'OJ- Field' in which four reservoir horizons were delineated. The reservoirs delineated show parallel to sub-parallel reflection patterns of the seismic events in general concordance with that of Agbada Formation in Niger Delta. The field is faulted with marked synthetic and antithetic faults which assisted in formation of roll-over anticlinal structures, and trapping of the migrating hydrocarbon from lower transgressive shale.

The four horizons are hydrocarbon bearing except in Sand\_B (OJ-02 and OJ-03 wells), Sand\_C (OJ-03 and OJ-04 wells) and Sand\_D (OJ-02 wells) that are wet with high porosity and permeability. Sand\_A is the most prolific hydrocarbon bearing with 56.07MMbbl of oil and recoverable reserve of 6.46MMbbl while Sand\_C is the second most prolific reservoir sand with 49.68MMbbl of oil and recoverable reserve of 11.92MMbbl. Sand\_D, which is the second least prolific, has 31.17MMbbl of oil, 112.74MMcf of gas and 0.94MMbbl recoverable reserve while the least prolific, Sand\_B, contain 26.05MMbbl of oil with recoverable reserve of 5.25MMbbl.

The OJ-01 well reservoir sands medium-fine grained, hydrocarbons bearing ( ODT) except Sand\_B that has an OWC with good porosity and permeability. It is the most promising of all the wells considered with 65.96MMbbl of oil and recoverable reserve of 5.21MMbbl. In OJ-02 well, Sand\_A (ODT) and Sand\_C (OWC) are hydrocarbon bearing with porosity and permeability range from 38 to 49% and 64.09 to 1145.56md. The OJ-02 well (Sand\_B and Sand\_D), is the second most promising for oil with 42.91MMbb and recoverable reserve of 13.63MMbbl. The OJ-03 also has two hydrocarbon bearing reservoirs (Sand\_A and Sand\_D) with low porosities of 32% and 34%. The permeability range from 138.76 to 520.57md with medium to fine grained sands. It is the least promising well with 13.52MMbbl of oil that yielded recoverable

reserve of 1.96MMbbl. In OJ-04 well, only Sand\_C is wet with water saturation of 59% and the remaining three reservoir sands are ideal for hydrocarbons accumulation with good contacts (ODT and gas-oil contact, GOC) and good recovery parameters. All the reservoir sands in OJ-04 well are medium to fine grained. Despite being wet, it is equally productive with 40.58MMbbl and 112.74MMcf of oil and gas and recoverable reserve of 3.77MMbbl.

Thus, most of the potential reservoir sands delineated show good petrophysical values and productivity. A total 162.98MMbbl of oil, 112.74MMcf of gas and 24.57MMbbl recoverable reserve is associated with a gross volume of 197255.92 acre-ft and net volume 96320.13 acre-ft of reservoir sands.

## References

- [1] Doust, H., and Omatsola, E. 1990. Niger Delta: In Edwards, J.D., and Santogrossi, P.A., (eds.), Divergent/passive margin basins: *American Association of Petroleum Geologists Memoir* 48: pp. 201-238.
- [2] Evamy, D., Haremboure, J., Kamerling, P., Knaap W. A., Molloy, F. A., and Rowlands, P. H. 1978. Hydrocarbon habitat of Tertiary Niger Delta. *American Association of Petroleum Geologists Bulletin*, Vol. 62, pp. 277-298.
- [3] Weber, K.J. and Daukoru, E.M. 1975. Petroleum geology of the Niger Delta: *Proceedings of the Ninth World Petroleum Congress, Geology*: London, Applied Science Publishers, Ltd. Vol. 2, 210-221.
- [4] Wu, S. and Bally, A.W. 2000. Slope tectonics – Comparisons and contrasts of structural styles of salt and shale tectonics of the northern Gulf of Mexico with shale tectonics of offshore Nigeria in Gulf of Guinea, in W. Mohriak and M. Talwani, eds., *Atlantic rifts and continental margins*; Washinton, D.C., American Geophysical Union, pp. 151 – 172.
- [5] Avbovbo, A.A. 1978. Tertiary litho-stratigraphy of Niger Delta: *American Association of Petroleum Geologists Bulletin*, Vol. 62, No. 2, pp. 295-300.

- [6] Ejedawe, J.E. 1981. Patterns of Incidence of Oil Reserves in Niger Delta Basin. *American Association of Petroleum Geologists Bulletin*, Vol. 65, pp. 1574-1585.
- [7] Weber, K.J. 1987. Hydrocarbon distribution patterns in Nigerian growth fault structures controlled by structural style and stratigraphy, *Journal of Petroleum Science and Engineering*, Vol. 1, pp. 91-104.
- [8] Edwards, J.D. and Santogrossi, P.A. 1990. Summary and conclusions, in Edwards, J.D., and Santogrossi, P.A., eds., *Divergent/passive Margin Basins*, *American Association of Petroleum Geologists*, Memoir 48: Tulsa, American Association of Petroleum Geologists, pp. 239-248.
- [9] Ekweozor, C.M. and Daukoru, E.M. 1992. The Northern Delta depobelt portion of the Akata-Agbada petroleum system, Niger Delta, Nigeria; *Nigerian Association of Petroleum Exploration Bulletin*, 72: pp. 102-120.
- [10] Beka, F.T. and Oti, M.N. 1995. The distal offshore Niger Delta: frontier prospects of a mature petroleum province. *Geology of Deltas*: Eds. Oti, M.N., Postma, G., Rotterdam, A.A. Balkema. pp. 237-241.
- [11] Kulke, H. 1995. Nigeria. *Regional Petroleum Geology of the World. Part II: Africa, America, Australia and Antarctica*, Eds. H. Kulke. Berlin: Gebruder Borntraeger. pp. 143-172.
- [12] Stacher, P. 1995. *Present understanding of the Niger Delta hydrocarbon habitat*. *Geology of Deltas*: Eds. Oti, M.N., Postma, G., Rotterdam, A.A. Balkema. pp. 257-267.
- [13] Smith-Rouch, L.S., Meisling, K.E., Hennings, P.E. and Armentrout, J.M. 1996. Tectono-stratigraphic computer experiments—Nigeria example: *American Association of Petroleum Geologists Bulletin*, Abstracts, May 1996.
- [14] Onuoha, K.M. 1999. Structural features of Nigeria's coastal margin: An assessment base of age data from wells: *Journal of African Earth Sciences*, Vol. 29, No. 3, pp. 485-499.
- [15] Nwachukwu, S.O. 1972. The tectonic evolution of the southern portion of the Benue Trough, Nigeria: *Geological Magazine*, Vol. 109, pp. 411-419.
- [16] Reijers, T.J.A., Petters, S.W. and Nwajide, C.S. 1997. The Niger Delta basin, in Selley, R.C., ed., *African basins*: Amsterdam, Elsevier Science, *Sedimentary Basins of the World* 3, pp. 151-172.
- [17] Short, K.C. and Stauble, A. J. 1965. Outline of geology of Niger Delta: *American Association of Petroleum Geologists Bulletin*, Vol. 51, pp. 761-779.
- [18] Bilotti, F.D., Shaw, J.H., Cupich, R.M. and Lakings, R.M. 2005. Detachment fold, Niger Delta, in Shaw, J.H., Connors, C. and Suppe, J., eds., *Seismic interpretation of contractional fault related folds: Studies in Geology American Association of Petroleum Geologists* Vol. 53, pp. 103-104.
- [19] Lawrence, S.R., Munday, S. and Bray, R. 2002. Regional geology and geophysics of the eastern Gulf of Guinea (Niger Delta to Rio Muni): *The Leading Edge*, Vol. 21, No. 11, pp. 1112-1117.
- [20] Bilotti, F.D. and Shaw, J.H. 2001. Modelling the compressive toe of the Niger delta as a critical taper wedge (abs.): *American Association of Petroleum Geologists. Annual Meeting Programme*, Vol. 10, pp. A18-A19.
- [21] Chatri, M. 1990. Enhanced resolution logging in Niger Delta. *Nigerian Association of Petroleum Explorationists Bulletin*, Vol. 5, pp. 52-74.
- [22] Morris, R.L. and Biggs, W.P. 1990. Using log derived values of water saturation and porosity. *SPWLA 8<sup>th</sup> Annual Logging Symposium*, pp. 1-26.
- [23] Crain, E.R., Garrido, M., Lamb, C. and Mosher, P. 2000. *Quantitative Analysis of Older Logs for Porosity and Permeability, Lake Maracaibo Western Flank Reservoirs*: Petrophysical Handbook. <http://www.spec2000.net>.
- [24] Schlumberger. 1998. *Log Interpretation Charts; Schlumberger Wireline and Testing*. Texas: Sugar Land. 122pp.
- [25] Hilchie, D.W. 1978. *Applied Openhole Log Interpretation*. D.W. Hilchie, Inc; Golden, CO. P.161.
- [26] Dresser Atlas. 1982. *Well Logging and Interpretation Techniques. The Course for Home Study*. Dresser Atlas Publication. P. 241.
- [27] Nelson, P.H. 1994. Permeability-porosity relationships in sedimentary rocks. *The Log Analyst*, pp. 38-62.